

On Discriminability and Diversity in Domain Adaptation

Shuhao Cui, Shuhui Wang, *Member, IEEE*, Junbao Zhuo, Liang Li, Qingming Huang, *Fellow, IEEE*, and Qi Tian, *Fellow, IEEE*

Abstract—In domain adaptation, the performance of classifier trained in source domain degrades when bumping into the high data density near the decision boundary in target domain. A common solution is to enhance the discriminability by directly minimizing the Shannon Entropy to push the decision boundary far away from the high density area. However, entropy minimization also leads to severe reduction of the prediction diversity, and unfortunately this side effect was mostly ignored in previous study. In this paper, we reinvestigate two critical issues in domain adaptation, *i.e.*, the prediction discriminability and diversity.

By studying the structure of the classification output matrix of a randomly selected data batch, we find by theoretical analysis that the prediction discriminability and diversity could be separately measured by the Frobenius-norm and rank of the batch output matrix. Meanwhile, the nuclear-norm is an upperbound of the Frobenius-norm, and a convex approximation of the matrix rank.

Accordingly, to improve both discriminability and diversity, we propose Batch Nuclear-norm Maximization (BNM) on the target output matrix. We further investigate Batch Nuclear-norm Minimization, to increase the knowledge applicability learned by source data.

To speed up the calculation of nuclear-norm, we reduce the computation complexity from $O(n^3)$ to $O(n^2)$ via approximation. Extensive experiments show that the proposed techniques could boost the adaptation procedure under three typical domain adaptation scenarios. The code is available at <https://github.com/cuishuhao/BNM>.

Index Terms—Domain adaptation, transfer learning, discriminability and diversity, computer vision.

1 INTRODUCTION

Deep neural networks have achieved great success in most computer vision applications. Nevertheless, it is well known that deep models in visual learning tasks largely rely on vast amounts of labeled data, where the labeling process is both expensive and time-consuming. Without sufficient amount of labeled training samples, as a common consequence, spurious predictions will be made, even with only a subtle departure from the training samples. Actually, in most applications, there exists large domain discrepancy between source and target data. To reduce such notorious domain discrepancy, researchers resort to Domain Adaptation (DA), which aims to enable knowledge transfer from labeled source domain to an unlabeled target domain. Recent advances in domain adaptation are mainly achieved by moment-alignment-based distribution matching [1], [2], [3] and adversarial learning [4], [5], [6].

Among a large number of DA models, it has been found that the transfer properties such as prediction discriminabil-

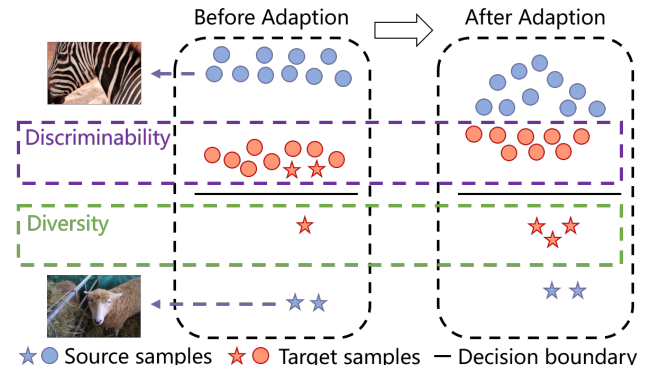


Fig. 1. Illustration of the transfer properties. Both prediction discriminability and diversity gain improvement after the adaptation procedure. More discriminability means less data near the decision boundary with overall reliable predictions, as shown in the dotted purple frame. Meanwhile, as shown in the dotted green frame, more diversity means more predictions on the minority category with few samples.

- Corresponding author: Shuhui Wang.
- S. Cui, S. Wang, J. Zhuo and L. Li are with the Key Laboratory of Intelligent Information Processing, Institute of Computing Technology, Chinese Academy of Sciences, Beijing 100190, China. S. Cui is also with the School of Computer Science and Technology, University of Chinese Academy of Sciences, Beijing 101408, China. E-mail: {cuishuhao18s, wangshuhui, liang.li}@ict.ac.cn, junbao.zhuo@vipl.ict.ac.cn}.
- Q. Huang is with the School of Computer Science and Technology, University of Chinese Academy of Sciences, Beijing 101408, China, with the Key Laboratory of Intelligent Information Processing, Institute of Computing Technology, Chinese Academy of Sciences, Beijing 100190, China and also with Peng Cheng Laboratory, Shenzhen 518066, China. E-mail: qmhuang@ucas.ac.cn.
- Q. Tian is with Cloud BU, Huawei Technologies, Shenzhen 518129, China. E-mail: tian.q1@huawei.com.

ity [7], [8] and diversity [9], [10] are the key that determines the overall cross-domain generalization ability, regardless of what backbone network used to construct the source model. For example, for the classification task, a good model is expected to produce highly confident predictions on examples from all the categories. Unfortunately, on target domain, the prediction discriminability is usually insufficient, due to the distribution divergence between source and target domains.

To reduce the uncertainty, a straightforward way is to minimize the Shannon Entropy to strengthen prediction discriminability on target domain [7], [8]. Meanwhile, to encourage the diversity, balance constraint [12] is devised

to equilibrate the distribution between different categories. Without distribution priors, the predicted pseudo-labels are adopted to calculate the statistical distribution in [9], [10], towards more predictions on the categories with less data instances.

However, the transfer properties are partially explored in existing methods. As shown in Figure 1, both discriminability and diversity should be enhanced after adaptation. Higher prediction discriminability means more reliable predictions, with less target data density near the decision boundary. The ambiguous target samples tend to be pushed into the nearby source samples, belonged to the majority categories with numerous samples. Thus the target samples, including the minority category samples, are prone to correspond to majority categories, with lessened prediction diversity. Higher diversity should be attained, to encourage predictions on minority categories. Existing balance constraint requires prior knowledge on minority categories, while the prior knowledge is always unavailable. Other methods approximate distribution knowledge by pseudo-labels, which seems less straightforward towards more accurate prediction.

In this paper, we reinvestigate the above issues, to enforce discriminability and diversity on the predictions of target data. We start by looking at the structure of classification output matrix of a randomly selected target data batch. We find by theoretical analysis that the discriminability and diversity can be measured by the Frobenius-norm and rank of the batch output matrix, respectively. The Frobenius-norm of a matrix can be bounded by the nuclear-norm of the matrix. Thus maximizing nuclear-norm ensures large Frobenius-norm of the batch matrix, with increased prediction discriminability. Meanwhile, the nuclear-norm of batch matrix is a convex approximation of the matrix rank, which refers to the prediction diversity. Accordingly, we propose Batch Nuclear-norm Maximization (BNM), an approach by maximizing the nuclear-norm of the batch output matrix to enhance both prediction discriminability and diversity.

Directing applying BNM to domain adaptation still faces three challenges, and we propose corresponding solutions. First, the knowledge learned by source domain might be difficult to transfer from. By analyzing the transfer properties on source domain, we formulate a novel method of Batch Nuclear-norm Minimization. The minimization process contributes to more effective source knowledge, mitigating the difficulties of transferring to target domain. Second, the calculation of singular value decomposition might not be converged in some cases, such as the experiments in Table 7. We approximate the calculation of nuclear-norm by the main components of $L_{1,2}$ -norm. The approximation can not only figure out the problem of convergence, but also speed up the training procedure with reduction of the computation complexity from $O(n^3)$ to $O(n^2)$. Third, BNM performs less effective in the situation with large amount of categories. We propose Multiple Batch Nuclear-norm Optimization, where we record the previous prediction matrices, and calculate nuclear-norm by multiple batch predictions. Extensive experiments validate the effectiveness of the proposed methods, under diverse domain adaptation scenarios.

This journal paper extends our previous work [13], with main extensions as follows. We extend BNM from the view

of transfer properties on source domain, and formulate a novel method of Batch Nuclear-norm Minimization. The calculation of nuclear-norm is further approximated by the main components of $L_{1,2}$ -norm. We also propose Multiple Batch Nuclear-norm Optimization, to overcome the situation with large amount of categories. In experiments, we construct a balanced dataset selected from Domainnet under unsupervised DA scenario. For diverse scenarios, we extend our methods to semi-supervised DA. We further insert our methods to recent method of HDAN [15] and SHOT [16]. Details can be found in summary of change.

Our contributions are summarized as follows:

- We theoretically prove that the discriminability and diversity of the prediction output can be measured by Frobenius-norm and rank of the batch output matrix.
- We propose Batch Nuclear-norm Maximization, a new learning paradigm that achieves better prediction discriminability and diversity on target domain.
- We propose Batch Nuclear-norm Minimization to construct easy-to-transfer knowledge on source domain.
- To speed up the calculation, we reduce the computation complexity of nuclear-norm from $O(n^3)$ to $O(n^2)$. Extensive experimental results validate the effectiveness of the proposed techniques and the flexibility to cooperate with existing methods.

2 RELATED WORK

Visual domain adaptation [17] has gained significant improvement in the past few years. Recently, domain adaptation (DA) methods focus on diverse adaptation circumstances, such as unsupervised DA [4], [13], [18], multi-source DA [19], [20], semi-supervised DA [21] and unsupervised open domain recognition [12]. While we explore the transfer properties in domain adaptation, to construct general frameworks suitable for various types of domain adaptation, similar to existing methods of [15], [18], [22].

In terms of distribution alignment, deep domain adaptation methods incorporate two main technologies into deep networks: moment alignment and adversarial training. Moment alignment methods [1], [3], [23] are devised with hand-crafted metrics, such as maximum mean discrepancy [1], [24], second-order statistics [2], [25] or other distance metrics of the representations [26]. Pioneered by Generative Adversarial Networks (GAN) [27], adversarial learning has been successfully explored on various tasks including domain adaptation. Domain adversarial neural network (DANN) [4], confuses the domain classifier by the gradient reversal layer, to lessen the domain shift. Then CyCADA [5] and CDAN [14] further devise adversarial frameworks inspired by powerful GANs. For individual domain adaptation, ADDA [28], MCD [6] and GVB [29] construct effective structures from the perspective of the minmax game.

Apart from distribution alignment, other adaptation methods optimize transfer properties by self training [30], [31] on target domain. The transfer properties mainly include prediction discriminability and diversity. To increase discriminability, Shannon Entropy [11] is directly minimized in [7], [8] to obtain reliable predictions for target samples. Entropy minimization is further modified into maximum

squares loss in [32], to reduce the influence of easy-to-transfer samples. Methods in [16], [33] calculate pseudo-labels on target domain, and further improve prediction discriminability by the cross entropy loss with pseudo-labels. Meanwhile, prediction discriminability is supposed to be lessened in [34] towards more transferability by penalizing the main components of the features. Higher prediction transferability is also achieved by smooth labeling in [35]. By harmonizing prediction transferability and discriminability, SAFN [18] is proposed by increasing the feature norm of target domain.

To maintain prediction diversity, a direct technique is to resort to imbalanced learning [36]. Existing imbalanced learning methods such as [12], [37] directly enforce the ratio of predictions on minority categories. However, the category distribution is required as prior knowledge. Without the prior knowledge, the prediction results are adopted as pseudo-labels in [9], [10], [30] to approximate the category distribution. Method in [16] increases prediction diversity by maximizing the mutual information between intermediate feature representations and outputs of the classifier. From another aspect of increasing diversity, Determinantal Point Processes (DPPs) [38] act probabilistically to capture the balance between quality and diversity within sets, but suffer from the large computation time. It deserves to stress that diversity is a more widespread problem compared with imbalanced learning due to two main reasons. On the one hand, prediction diversity might still be reduced under balanced situations, as discussed in Table 1. On the other hand, category imbalance is a problem in common datasets, while diversity is a property on the predictions and generations. Ensuring diversity is a solution for a widely adopted machine learning problem of mode collapse [39].

In this paper, we analyze the problem from the perspective of matrix analysis [40], [41], which has already been widely applied to numerous computer vision tasks, such as image denoising [42] and image restoration [43]. Among the tasks, a common assumption is that the noisy data brings extra components to the matrix. To reduce the influence of the extra components, minimizing nuclear-norm of the matrix has been widely accepted in [42], [43]. In comparison to the above methods, we aim to explore the residual parts in target domain. Thus in our method, the nuclear-norm of the target response matrix is maximized towards high prediction diversity. Recently, BSP [34] penalizes the largest singular values of the feature matrix to boost prediction discriminability. While we analyze the batch classification response matrix to promote both the prediction discriminability and diversity.

3 METHOD

3.1 Discriminability and Diversity

More prediction discriminability means less ambiguous target samples near the task-specific decision boundary. The ambiguous samples tend to be misclassified, thus increased prediction discriminability could ensure reliable predictions. Meanwhile, we reanalyze popular method of SAFN [18] as shown in Figure 2. The blue line of SAFN indicates that the intrinsic effect of SAFN is to increase the

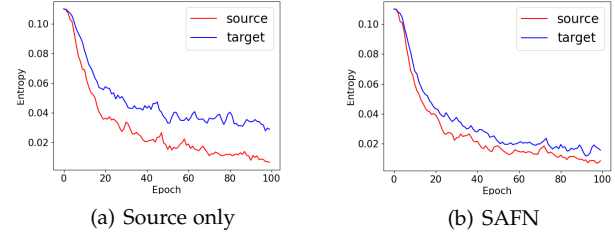


Fig. 2. Statistics of Entropy during the whole training process under Source only or SAFN. Less Entropy means more prediction discriminability for the method.

TABLE 1
Ratio(%) of categories with different sample numbers in the batch.

Number	0	1	2	≥ 3
$B = 0.5C$	60.4	30.7	7.5	1.4
$B = C$	36.4	37.2	18.6	7.8
$B = 2C$	12.9	27.2	27.6	32.3

feature norm towards more prediction discriminability. Discussion can be found in Supplementary, from the theoretical and practical perspectives in detail.

It is normal in randomly selected batch B samples to be imbalanced, even sampled from a balanced dataset. In a balanced dataset with categories $C = 126$, we show the ratio of categories with difference number of samples under different batch size B in Table 1. When B equals C , more than one third of categories are ignored with no samples in the batch. Predictions on ignored categories, denoted as minority categories tend to be damaged during the optimization of the batch. Meanwhile, 7.8% categories attain more than 3 samples in the batch, denoted as majority categories. The majority categories tend to dominate the succeeding prediction matrices. Even in $B = 2C$, there are still 12.9% categories ignored in the batch, which validates the degradation on prediction diversity in balanced dataset. In this case, directly increasing discriminability tends to classify the ambiguous samples to the majority categories. The continuous convergence to the majority categories results in lessened prediction diversity.

To investigate the transfer properties in domain adaptation, we start by looking at the prediction outputs on a data batch with B randomly selected samples. We denote the number of categories as C , and the batch prediction output matrix as $A \in \mathbb{R}^{B \times C}$, which satisfies:

$$\sum_{j=1}^C A_{i,j} = 1 \quad \forall i \in 1 \dots B \\ A_{i,j} \geq 0 \quad \forall i \in 1 \dots B, j \in 1 \dots C, \quad (1)$$

where deep methods can attain satisfying response matrix A , under enormous labeled samples.

3.1.1 Discriminability Measurement: F -norm

Higher discriminability means less prediction uncertainty in the response matrix A . To measure the uncertainty, most methods resort to Shannon Entropy [11], denoted as entropy for simplicity. Entropy could be calculated as follows:

$$H(A) = -\frac{1}{B} \sum_{i=1}^B \sum_{j=1}^C A_{i,j} \log(A_{i,j}). \quad (2)$$

For more discriminability, we could directly minimize $H(A)$, the same as [7], [8], [44]. When $H(A)$ reaches the minimum, only one entry is 1 and the other $C - 1$ entries are 0 in each row of A , *i.e.*, $A_{i,j} \in \{0, 1\} \quad \forall i \in 1 \dots B, j \in 1 \dots C$. The minimum exactly satisfies the highest prediction discriminability of A , where each prediction in A_i is fully determined.

By enforcing A to the same value with minimum in $H(A)$, other functions could also improve prediction discriminability. We choose to calculate Frobenius-norm (F -norm) $\|A\|_F$ as follows:

$$\|A\|_F = \sqrt{\sum_{i=1}^B \sum_{j=1}^C |A_{i,j}|^2}. \quad (3)$$

Theorem 1. Given matrix A , $H(A)$ and $\|A\|_F$ have strict opposite monotonicity about the values of matrix A .

The proof can be found in Supplementary. According to the theorem, the minimum of $H(A)$ and the maximum of $\|A\|_F$ could be achieved at the same value of A . Particularly, the upper-bound of $\|A\|_F$ can be calculated according to inequality of arithmetic and geometric means, as follows:

$$\begin{aligned} \|A\|_F &\leq \sqrt{\sum_{i=1}^B \left(\sum_{j=1}^C A_{i,j} \right) \cdot \left(\sum_{j=1}^C A_{i,j} \right)} \\ &= \sqrt{\sum_{i=1}^B 1 \cdot 1} = \sqrt{B}. \end{aligned} \quad (4)$$

The upper-bound of $\|A\|_F$ will be reached along with the minimum of $H(A)$. Thus less uncertainty and more prediction discriminability would be attained, if $\|A\|_F$ is maximized.

Meanwhile, we could minimize $\|A\|_F$ towards lessened prediction discriminability. The lower-bound of $\|A\|_F$ could be calculated as:

$$\begin{aligned} \|A\|_F &\geq \sqrt{\sum_{i=1}^B \frac{1}{C} \cdot \left(\sum_{j=1}^C A_{i,j} \right) \cdot \left(\sum_{j=1}^C A_{i,j} \right)} \\ &= \sqrt{\sum_{i=1}^B \frac{1}{C} \cdot 1 \cdot 1} = \sqrt{\frac{B}{C}}, \end{aligned} \quad (5)$$

where the minimum could be reached when $A_{i,j}$ equals $\frac{1}{C}$ for each i and j . The circumstance satisfies the same prediction probabilities for all the C categories, with least prediction discriminability.

3.1.2 Diversity Measurement: Matrix Rank

Higher prediction diversity means more involved categories in matrix A . For a certain dataset, the number of predicted categories in A is expected to be a constant on average, denoted as E_C . To provide intuitive comprehension of E_C , we construct a toy dataset, with only 2 samples separately belonging to 2 categories. We randomly select 2 samples, and the samples hold 0.5 probability of belonging to only 1 category, and the other 0.5 probability of belonging to 2 categories. Then the constant E_C could be calculated by:

$$E_C = 0.5 \times 1 + 0.5 \times 2 = 1.5, \quad (6)$$

where the matrix is expected to contain 1.5 categories on average.

Generally speaking, the predicted constant E_C is the expectation of category number $C_p(A)$ for multiple A selected from domain \mathcal{D} , as follows:

$$E_C = \mathbb{E}_{A \sim \mathcal{D}}(C_p(A)). \quad (7)$$

For well-performed predictions, E_C should be similar to the average ground truth category number for all A . Under certain selection mode, the ground truth category number should be a constant on average. Thus the predicted category number E_C should also be a constant. If the constant E_C becomes larger, more categories are involved with higher prediction diversity. Thus, for existing batch matrix A , prediction diversity could be measured by predicted category number $C_p(A)$. $C_p(A)$ could be calculated by counting the number of predicted categories on the one-hot matrix. The number of components is called the matrix rank, while one-hot matrix is accomplished by the argmax operation, as follows:

$$C_p(A) = \text{rank}(\mathbb{I}[A_{i,\text{arg max}(A_i)}]). \quad (8)$$

However, the argmax operation could not propagate the gradient of the loss functions. Thus we further analyze the relationship between category number $C_p(A)$ and the predicted vectors in A . Two randomly selected prediction vectors, *i.e.*, A_i and A_k , could be linearly independent when A_i and A_k belong to different categories. When A_i and A_k belong to the same category and $\|A\|_F$ is near \sqrt{B} , the differences between A_i and A_k are tiny. Then A_i and A_k could be approximately regarded as linearly dependent. The largest number of linear independent vectors is called the matrix rank. Thus, $\text{rank}(A)$ could be an approximation of $C_p(A)$, if $\|A\|_F$ is near the upper-bound \sqrt{B} , as follows:

$$C_p(A) \approx \text{rank}(A) \quad (9)$$

Apparently, the maximum value of $C_p(A)$ is $\min(B, C)$. When $B \geq C$, the maximum value is C , which firmly guarantees that the prediction diversity for the batch achieves the maximum. However, when $B < C$, the maximum value is less than C , maximization of $C_p(A)$ still enforces that the predictions on the batch samples should be as diverse as possible, though there is no guarantee that all the categories will be assigned to at least one example. Therefore, maximization of $C_p(A)$ could ensure the diversity in any case.

3.2 Batch Nuclear-norm

3.2.1 Discriminability and Diversity in Batch Nuclear-norm

For a normal matrix, the calculation of the matrix rank is a NP-hard non-convex problem. Thus we could not directly restrain the rank of matrix A . To explore the diversity in matrix A , we are supposed to find the relationship between $\text{rank}(A)$ and nuclear-norm.

Theorem 2. When $\|A\|_F \leq 1$, the convex envelope of $\text{rank}(A)$ is the nuclear-norm $\|A\|_*$.

The theorem is proved in [45]. In our settings, different from above theorem, we have $\|A\|_F \leq \sqrt{B}$ as shown in Eqn. 4. Thus the convex envelope of $\text{rank}(A)$ becomes $\|A\|_* / \sqrt{B}$,

which is also proportional to $\|A\|_*$. Meanwhile, $\text{rank}(A)$ can approximately indicate the diversity, when $\|A\|_F$ is near the upper-bound, as described in Sec. 3.1.2. Therefore, if $\|A\|_F$ is near \sqrt{B} , prediction diversity can be approximately represented by $\|A\|_*$. Therefore, maximizing $\|A\|_*$ ensures higher prediction diversity.

For matrix A, nuclear-norm $\|A\|_*$ is defined as the sum of singular values of A, calculated as follows:

$$\|A\|_* = \sum_{i=1}^D \sigma_i, \quad (10)$$

where σ_i denotes the i th largest singular value. The number of the singular values is denoted as D , the smaller one in B and C , i.e., $D = \text{Min}(B, C)$. For batch prediction output matrix A, $\|A\|_*$ is called batch nuclear-norm.

To explore the discriminability in $\|A\|_*$, we are supposed to analyze the relationship between $\|A\|_*$ and $\|A\|_F$. We find that $\|A\|_F$ can be also expressed by singular values σ_i follows:

$$\|A\|_F = \sqrt{\sum_{i=1}^D \sigma_i^2}, \quad (11)$$

where the calculation is shown in Supplementary in detail. With auxiliary singular values, the relationship between $\|A\|_*$ and $\|A\|_F$ is demonstrated as follows:

$$\frac{1}{\sqrt{D}} \|A\|_* \leq \|A\|_F \leq \|A\|_* \leq \sqrt{D} \cdot \|A\|_F, \quad (12)$$

with the same conclusion with [45], [46], [47], where $\|A\|_*$ and $\|A\|_F$ could bound each other. Therefore, $\|A\|_F$ tends to be larger, if $\|A\|_*$ becomes larger. Since maximizing $\|A\|_F$ could increase the discriminability described in Sec. 3.1.1, maximizing $\|A\|_*$ also contributes to the improvement on prediction discriminability.

Due to the relationship between $\|A\|_*$ and $\|A\|_F$ in Eqn. 13, and the fact that upper-bound of $\|A\|_F$ is \sqrt{B} in Eqn. 4, we calculate the maximum of $\|A\|_*$ as follows:

$$\|A\|_* \leq \sqrt{D} \cdot \|A\|_F \leq \sqrt{D \cdot B}, \quad (13)$$

where the two inequality conditions in the equation correspond to the two influence factors of $\|A\|_*$ respectively. The first inequality corresponds to the diversity, and the second to the discriminability. When prediction diversity is higher, the rank of A tends to be larger with increased $\|A\|_*$. Similarly, high prediction discriminability accompanies with increased $\|A\|_F$ and large $\|A\|_*$.

3.2.2 Fast Batch Nuclear-norm

To obtain the nuclear-norm, we are supposed to calculate all the singular values in the matrix A. The singular value decomposition computed on the matrix $A \in \mathbb{R}^{B \times C}$ costs $O(\min(B^2C, BC^2))$ time. The computation complexity could be simply denoted as $O(n^3)$, where n is the variable scale. In normal circumstance, B and C are small, and the overall computational budget of $\|A\|_*$ is almost negligible in the training of deep networks. However, when B and C are large, the computation complexity is large and the calculation of $\|A\|_*$ is time-consuming. Besides, the calculation of singular value decomposition might not be

converged in some cases, such as the experiments in Table 7. Thus we seek for approximations of the singular values towards fast and efficient calculation.

The singular values σ_i are the main components of the matrix A. In sample A_i , only a few categories are corresponding, and the responses to the rest categories are 0. Thus matrix A should be sparse, and the singular values of A could be approximated by the combination of category responses in A.

Theorem 3. If $\|A\|_F$ is near the upper-bound \sqrt{B} , the i th biggest singular value σ_i can be approximated by:

$$\sigma_j \approx \text{top}(\sum_{i=1}^B A_{i,j}^2, j) \quad \forall i \in 0, \dots, D. \quad (14)$$

The theorem is proved in Supplementary. With approximation of the singular values, we calculate the batch nuclear-norm in a fast way, as follows:

$$\|\hat{A}\|_* = \sum_{j=1}^D \text{top}(\sqrt{\sum_{i=1}^B A_{i,j}^2}, j) \quad (15)$$

where the method is called Fast Batch Nuclear-norm, as the fast version of nuclear-norm. The equation means that in terms of A, the main components of the $L_{1,2}$ -norm could approximate nuclear-norm, if $\|A\|_F$ is near the upper-bound \sqrt{B} . While the rest entries of the $L_{1,2}$ -norm are regarded as noisy parts in response matrix A.

Fast Batch Nuclear-norm maintains two advantages compared with original nuclear-norm. On the one hand, the computation complexity of $\|\hat{A}\|_*$ is $O(\min(BC, B^2))$, denoted as $O(n^2)$ for simplify. From the math view, Fast Batch Nuclear-norm reduces the computation complexity from $O(n^3)$ to $O(n^2)$, and speeds up the calculation process. On the other hand, $\|\hat{A}\|_*$ is based on the calculation of singular value decomposition, and singular value decomposition might not be converged in some cases. While the computation of the fast version $\|\hat{A}\|_*$ is based on directly combining matrix components, without concerns on not converging.

3.2.3 Extreme Points in Batch Nuclear-norm

Based on the above discovery, maximizing $\|A\|_*$ attains improvement on both prediction discriminability and diversity. For better comprehension of Batch Nuclear-Norm, we construct a toy examples to demonstrate the extreme points.

We assume B and C are 2. In this case, A could be expressed as:

$$A = \begin{bmatrix} x & 1-x \\ y & 1-y \end{bmatrix}, \quad (16)$$

where x and y are variables. Thus negative entropy, F-norm, nuclear-norm and fast nuclear-norm could be calculated as:

$$\begin{aligned} -H(A) &= x \log(x) + (1-x) \log(1-x) + y \log(y) \\ &\quad + (1-y) \log(1-y) \\ \|A\|_F &= \sqrt{x^2 + (1-x)^2 + y^2 + (1-y)^2} \\ \|A\|_* &= \sqrt{x^2 + (1-x)^2 + y^2 + (1-y)^2 + 2|y-x|} \\ \|\hat{A}\|_* &= \sqrt{x^2 + (1-x)^2} + \sqrt{y^2 + (1-y)^2}, \end{aligned} \quad (17)$$

where the calculation of $\|A\|_*$ is described in Supplementary. For entropy and F -norm, there is no constraint on the relationship between x and y , thus negative entropy and F -norm could reach the maximum when:

$$A = \begin{bmatrix} 1 & 0 \\ 1 & 0 \end{bmatrix}, \begin{bmatrix} 0 & 1 \\ 1 & 0 \end{bmatrix}, \begin{bmatrix} 1 & 0 \\ 0 & 1 \end{bmatrix}, \begin{bmatrix} 0 & 1 \\ 0 & 1 \end{bmatrix}. \quad (18)$$

But $\|A\|_*$ and $\|\hat{A}\|_*$ will reach the maximum only when:

$$A = \begin{bmatrix} 0 & 1 \\ 1 & 0 \end{bmatrix}, \begin{bmatrix} 1 & 0 \\ 0 & 1 \end{bmatrix}, \quad (19)$$

where $\|A\|_*$ and $\|\hat{A}\|_*$ enforce diversity by maximizing the prediction divergences among the batch data. The maximum of $\|\hat{A}\|_*$ is calculated in Supplementary. Meanwhile, the measurements will reach minimum if and only if:

$$A = \begin{bmatrix} 0.5 & 0.5 \\ 0.5 & 0.5 \end{bmatrix}, \quad (20)$$

which satisfies the situation with least prediction discriminability and diversity (equal prediction probabilities result in only one category prediction).

3.3 Batch Nuclear-norm for Domain Adaptation

In domain adaptation, we are given source domain \mathcal{D}_S and target domain \mathcal{D}_T . There are N_S labeled source samples $\mathcal{D}_S = \{(x_i^S, y_i^S)\}_{i=1}^{N_S}$ in C categories and N_T unlabeled target samples $\mathcal{D}_T = \{x_i^T\}_{i=1}^{N_T}$ in the same C categories. In \mathcal{D}_S , the labels are denoted as $y_i^S = [y_{i1}^S, y_{i2}^S, \dots, y_{iC}^S] \in \mathbb{R}^C$, where y_{ij}^S equals to 1 if x_i^S belongs to the j th category otherwise 0.

For object recognition, the classification responses are acquired by deep network G , i.e., $A_i = G(x_i)$. Network G consists of a feature extraction network, a classifier and a softmax layer. With randomly sampled batch B_S samples $\{X^S, Y^S\}$ on the source domain, the classification loss on \mathcal{D}_S could be calculated as:

$$\mathcal{L}_{cls} = \frac{1}{B_S} \left\| Y^S \log(G(X^S)) \right\|_1, \quad (21)$$

where $\|Y^S \log(G(X^S))\|_1$ denotes the L_1 -norm. The classification loss on source domain provides initial parameters for further optimization.

3.3.1 Batch Nuclear-norm Maximization and Minimization

On target domain \mathcal{D}_T , with randomly sampled batch B_T examples $\{X^T\}$, the classification response matrix could be denoted as $G(X^T)$. To improve both the prediction discriminability and diversity, we propose Batch Nuclear-norm Maximization (BNMax) by maximizing the nuclear-norm of the batch matrix $G(X^T)$ on target domain. The loss function of BNMax, denoted as \mathcal{L}_{BNMax} can be formulated as:

$$\mathcal{L}_{BNMax} = -\frac{1}{B_T} \left\| G(X^T) \right\|_*, \quad (22)$$

where the neural network G is shared between \mathcal{D}_S and \mathcal{D}_T . Minimizing \mathcal{L}_{BNMax} reduces the target data density near the decision boundary without diversity degradation. With maintained prediction diversity, more reliable predictions are gained, compared with entropy minimization.

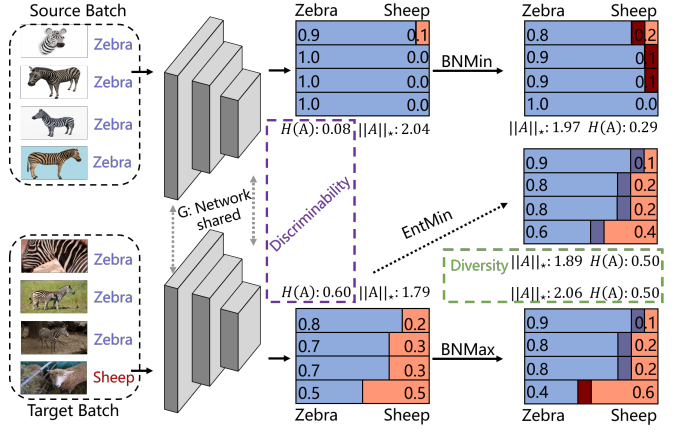


Fig. 3. Illustration of the framework of Batch Nuclear-norm Maximization and Minimization (BNM^2), which composed of BNMin and BNMax in a toy example of 4 batch size and 2 categories. The dark region means the variance of the variable, i.e., the dark blue (red) represents the increase of blue (red) variable. $H(A)$ represents the entropy value and the value of nuclear-norm is denoted as $\|A\|_*$.

On source domain \mathcal{D}_S , the classification response matrix of sampled batch B_S examples $\{X^S\}$ is denoted as $G(X^S)$. The overly confident source predictions $G(X^S)$ indicates that $G(X^S)$ might be overfitting to source domain, resulting in difficulties for adapting to target domain. Thus to lessen the prediction discriminability, we propose Batch Nuclear-norm Minimization (BNMin) by minimizing nuclear-norm of $G(X^S)$ on source domain. The loss function of BNMin, denoted as \mathcal{L}_{BNMin} can be calculated as:

$$\mathcal{L}_{BNMin} = \frac{1}{B_S} \left\| G(X^S) \right\|_*. \quad (23)$$

Minimizing \mathcal{L}_{BNMin} could reduce the distance from source data to the decision boundary, with less prediction discriminability on source domain. The key insight of BNMin is to prevent overfitting on source data, for more generalized knowledge learned by source domain.

The gradient of nuclear-norm could be calculated according to [48], thus \mathcal{L}_{BNMax} and \mathcal{L}_{BNMin} could be directly applied to the end-to-end training process for gradient-based deep networks. To train the network, we simultaneously optimize classification loss, BNMax loss and BNMin loss. Thus \mathcal{L}_{cls} , \mathcal{L}_{BNMax} and \mathcal{L}_{BNMin} , combined with the parameter λ , can be optimized as follows:

$$\begin{aligned} \mathcal{L}_{BNM} &= \mathcal{L}_{cls} + \lambda \cdot (\mathcal{L}_{BNMax}), \\ \mathcal{L}_{BNM^2} &= \mathcal{L}_{cls} + \lambda \cdot (\mathcal{L}_{BNMin} + \mathcal{L}_{BNMax}), \end{aligned} \quad (24)$$

where method with Batch Nuclear-norm Maximization is denoted as BNM (\mathcal{L}_{BNM}), Batch Nuclear-norm Maximization and Minimization is denoted as BNM^2 (\mathcal{L}_{BNM^2}). When Batch Nuclear-Norm is replaced by Fast Batch Nuclear-norm, the loss functions with Eqn. 10 are replaced by Eqn. 15. Then the loss functions of Fast Batch Nuclear-norm Maximization, Fast Batch Nuclear-norm Maximization and Minimization are respectively denoted as FBNM and $FBNM^2$ in short.

By enforcing diversity, the key insight of BNM is sacrificing a certain level of the target prediction hit-rate on majority categories, to enhance the prediction hit-rate on minority

categories. The samples belonging to the majority classes might be misclassified as minority classes, to increase the diversity. Fortunately, the classification loss \mathcal{L}_{cls} on source domain would penalize the wrongly encouraged diversity for target predictions, since model G is shared between source and target domain. Asymptotically, model G tends to produce more diverse target predictions, given that the samples can be correctly predicted. The majority categories tend to dominate the predictions of target batch samples, while BNMax is effective to avoid prediction degradation for domain adaptation under both balanced and imbalanced category distributions.

To provide comprehensive understanding of our methods, we show a toy example in Figure 3. We assume that there are only two categories, *i.e.*, zebra and sheep. There are 4 zebras as source batch, and 3 zebras and a goat in target batch, with zebra as the majority category. There exists large discriminability discrepancy on the measurement of $H(A)$, from 0.08 to 0.60 for initial values. The discrepancy gap is lessened by both BNMin on source batch, and BNMax on target batch. As the key role in our method, BNMax could ensure both the prediction discriminability and diversity for target domain. Higher prediction discriminability is represented by larger $H(A)$ after adaptation. Meanwhile, the improvement on diversity is shown by larger $\|A\|_*$ under the same $H(A)$, compared with EntMin.

3.3.2 Multi Batch Nuclear-norm Optimization

In some cases, the category number C is quite large, then batch size B should not be negligible small during the training procedure. However, large B and C might be difficult to calculate, due to the limitation of devices. Thus we seek for solutions for the circumstance of large C and small B .

To mitigate the problem of small B , we record the predictions of A for further optimization. We record K previous prediction matrices by concatenating the matrices into a large matrix R , with manually set parameter K . With enough K records, we calculate BNMax and BNMin loss functions based on R . For the K matrices, only the K th matrix propagates the gradient of the loss functions. After the gradient propagation, the K matrices are cleared up, to provide room for further prediction records R . The optimization process of BNM² with matrix R is shown in Algorithm 1. When K is large enough, matrix R could contain predictions for the whole dataset. When K is 1, the optimization process is the same with the calculation in BNM². When multiple BNMax is adopted, Line 5 in Algorithm 1 is replaced with \mathcal{L}_{BNM} . Fast BNM and fast BNM² could also be equipped with multiple optimization, by replacing the nuclear-norm in the algorithm by fast versions in Eqn. 15.

4 EXPERIMENTS

We apply our method to three domain adaptation situations, *i.e.*, unsupervised domain adaptation (UDA), semi-supervised domain adaptation (SSDA), and unsupervised open domain recognition (UODR). The experiments of the three tasks are accomplished on datasets of Office-31 [17], Office-Home [49], Balance Domainnet, Semi Domainnet [21]

Algorithm 1 Multi Batch Nuclear-norm

Input: network G , selected source data X_i^S and target data X_i^T for i th iteration, with total M iterations, multiple num K and record value for source R^S and target R^T .

Output: network weights of G .

```

1:  $R^S, R^T = [ ], [ ]$ 
2: for  $i = 1$  to  $M$  do
3:    $\mathcal{L} = \frac{1}{B_S} \|Y^S \log(G(X^S))\|_1$ 
4:   if  $i \% K = 0$  then
5:      $\mathcal{L} += \frac{1}{B_S} \|[G(X^S); R^S]\|_* - \frac{1}{B_T} \|[G(X^T); R^T]\|_*$ 
6:    $R^S, R^T = [ ], [ ]$ 
7:   else
8:      $R^S = [G(X^S); R^S]$ 
9:      $R^T = [G(X^T); R^T]$ 
10:   end if
11:   Update  $G$ .
12: end for

```

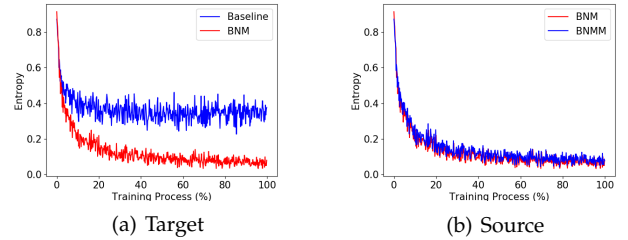


Fig. 4. Prediction discriminability for Ar → Cl. As a typical measurement, less entropy means more prediction discriminability.

and I2AwA [12]. We also denote the direct entropy minimization, batch Frobenius-norm maximization as EntMin, BFM in our experiments. When BNM and other methods cooperate with existing methods, we connect the method names with “+”.

4.1 Unsupervised Domain Adaptation

Office-31 [17] and Office-Home [49] are standard benchmarks for unsupervised domain adaptation. Office-31 contains 4,110 images in 31 categories, and consists of three domains: Amazon (A), Webcam (W), and DSLR (D). We evaluate the methods across the three domains, resulting in six transfer scenarios. Office-Home is a relative challenging dataset with 15,500 images in 65 categories. It has four significantly different domains: Artistic images (Ar), Clip Art (Cl), Product images (Pr), and Real-World images (Rw). There are 12 challenging transfer tasks among four domains in total.

We adopt ResNet-50 [50] pre-trained on ImageNet [56] as our backbone. The batch size is fixed to be 36 in our experiments, implemented with PyTorch [57]. During the training of the network, we employ mini-batch stochastic gradient descent (SGD) with initial learning rate as 0.0001 and momentum of 0.9 to train our model. When BNM is regarded as a typical method, the parameter λ is fixed to be 0.5. When BNM is combined with existing methods, the parameter λ is set to be 0.25. For each method, we run four random experiments and report the average accuracy, to obtain reliable performance.

TABLE 2
Accuracies (%) on Office-31 for ResNet50-based unsupervised domain adaptation methods.

Method	A	D	A	W	D	W	W	D	D	A	W	A	Avg
ResNet-50 [50]	68.9	68.4	96.7	99.3	62.5	60.7	76.1						
GFK [51]	74.5	72.8	95.0	98.2	63.4	61.0	77.5						
DAN [1]	78.6	80.5	97.1	99.6	63.6	62.8	80.4						
DANN [4]	79.7	82.0	96.9	99.1	68.2	67.4	82.2						
ADDA [28]	77.8	86.2	96.2	98.4	69.5	68.9	82.9						
MaxSquare [32]	90.0	92.4	99.1	100.0	68.1	64.2	85.6						
Simnet [52]	85.3	88.6	98.2	99.7	73.4	71.8	86.2						
GTA [53]	87.7	89.5	97.9	99.8	72.8	71.4	86.5						
MCD [6]	92.2	88.6	98.5	100.0	69.5	69.7	86.5						
CBST [9]	86.5	87.8	98.5	100.0	70.9	71.2	85.8						
CRST [10]	88.7	89.4	98.9	100.0	70.9	72.6	86.8						
EntMin	86.0	87.9	98.4	100.0	67.0	63.7	83.8						
BFM	87.7	86.9	98.5	100.0	67.6	63.0	84.0						
BNM	90.3	91.5	98.5	100.0	70.9	71.6	87.1						
FBNM	90.4	91.9	98.6	99.9	71.2	70.5	87.1						
BNM ²	92.6	92.6	98.7	99.9	72.4	73.6	88.3						
FBNM ²	91.6	92.7	98.5	100.0	72.1	73.1	88.0						
CDAN [14]	92.9	93.1	98.6	100.0	71.0	69.3	87.5						
CDAN+EntMin	92.0	91.2	98.7	100.0	70.7	71.0	87.3						
CDAN+BNM	92.9	92.8	98.8	100.0	73.5	73.8	88.6						
CDAN+FBNM	92.7	92.4	98.6	99.7	74.0	73.7	88.5						
CDAN+BNM ²	93.4	92.7	99.0	100.0	73.5	75.5	89.0						
CDAN+FBNM ²	92.6	92.4	99.0	100.0	74.7	74.2	88.8						
SHOT [16]	94.0	90.1	98.4	99.9	74.7	74.3	88.6						
BNM-S	93.0	93.0	98.2	99.9	75.4	74.9	89.1						
FBNM-S	93.0	92.9	98.2	99.9	75.4	75.0	89.1						

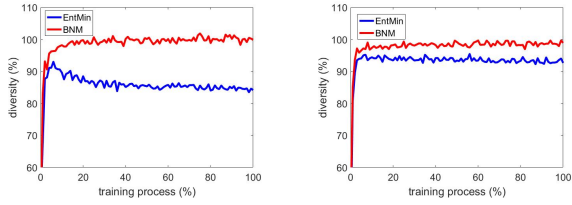


Fig. 5. Diversity ratio on Office-Home for domain adaptation, calculated as the predicted diversity divided by the ground truth diversity. The predicted (ground truth) diversity is measured by the average number of predicted (ground truth) categories in randomly sampled batches.

The results on Office-31 and Office-Home are shown in Table 2 and 3. On both Office-31 and Office-Home, as expected, BFM obtains similar results with EntMin, while BNM achieves substantial improvement on average over other entropy-based methods. Surprisingly, BNM obtains superior results compared with popular alignment-based competitors. The results show that Batch Nuclear-norm Maximization is effective for domain adaptation, especially on the difficult tasks where the baseline accuracy is relatively low, such as D→A in Office-31 and Rw→Cl in Office-Home. Beyond typical BNM, we also construct framework of BNM², which achieves remarkable improvement, compared with BNM. Meanwhile, the approximated method FBNM achieves similar results with BNM. FBNM² further achieves similar results compared with BNM². The results show that our fast approximation method of nuclear-norm is suitable to replace original calculation of nuclear-norm in optimizations of both BNMax and BNMin.

Meanwhile, we add BNM and BNM² to existing methods of CDAN [14] and HDAN [15], denoted as CDAN+BNM, CDAN+BNM², HDAN+BNM and

HDAN+BNM² respectively. In terms of the performance, CDAN+BNM outperforms CDAN and CDAN+EntMin by a large margin on both Office-31 and Office-Home. Besides, HDAN+BNM performs better than HDAN on Office-Home, which also shows that BNM could cooperate well with other methods. BNM is more suitable to improve the performance of CDAN and HDAN on the difficult tasks where the baseline accuracy is relatively low, such as D→A and W→A in Office-31, Ar→Cl and Pr→Cl in Office-Home. In cooperation with CDAN and HDAN, BNM² could still outperform BNM on both Office-31 and Office-Home, which shows the necessity of BNMin. We also replace the methods of BNM and BNM² by FBNM and FBNM². The approximation methods of FBNM and FBNM² achieve similar results compared with BNM and BNM², which shows the effectiveness of the approximation.

Recent work of SHOT [16] achieves well-performed results, with similar constraint compared with BNM. Thus we reproduce the results of BNM under the same environment with SHOT. Since source data is not utilized in the training of SHOT, we could not apply BNM² to the framework. We replace the constraint on prediction diversity of information maximization by BNM, and FBNM, denoted as BNM-S and FBNM-S respectively. The reproduced results are shown in Table 2 and 3, which shows BNM-S could also outperform SHOT on average on both Office-31 and Office-Home. Specifically, BNM-S and FBNM-S could achieve obvious improvement than SHOT on difficult tasks, such as D→A in Office-31 and Rw→Cl in Office-Home. The results show that simply limiting prediction discriminability and diversity by BNM is enough for most cases.

To analyze prediction discriminability for domain adaptation in BNM, we calculate the typical measurement of entropy, as shown in Figure 4. Compared with the baseline of source only, BNM achieves less entropy and more prediction discriminability for target domain, as shown in Figure 4(a) during most of the training process. On source domain, as shown in Figure 4(b), BNM² could lessen prediction discriminability on source domain compared with BNM. Though the differences seem to be little in the figure, the differences are still considerable, under the explicit constraint of cross entropy loss on source domain.

To validate that BNM could maintain diversity in domain adaptation, we show the diversity ratio in Office-Home on tasks of Ar → Cl and Ar → Pr in Figure 5. Prediction diversity is measured by the average matrix rank, i.e., mean number of predicted categories in randomly sampled batch. Thus the diversity ratio is measured by the average predicted category number dividing the average ground-truth category number. As shown in Figure 5(a), the diversity ratio of BNM is larger than that of the EntMin by a large margin in Ar → Cl. The phenomenon is reasonable since the rich samples near the decision boundary are mainly classified into the majority categories, reducing the diversity in the batch examples. As shown in Figure 5(b), the diversity ratio of BNM is still larger than that of the EntMin in Ar → Pr. But in Ar → Pr, the divergence between EntMin and BNM in diversity ratio is less than the divergence in Ar → Cl. The lessened diversity differences result from fewer samples near the decision boundary in Ar → Pr. Less ambiguous samples in Ar → Pr could be explained

TABLE 3
Accuracies (%) on Office-Home for ResNet50-based unsupervised domain adaptation methods.

Method	Ar → Cl	Ar → Pr	Ar → Rw	Cl → Ar	Cl → Pr	Cl → Rw	Pr → Ar	Pr → Cl	Pr → Rw	Rw → Ar	Rw → Cl	Rw → Pr	Avg
ResNet-50 [50]	34.9	50.0	58.0	37.4	41.9	46.2	38.5	31.2	60.4	53.9	41.2	59.9	46.1
DAN [1]	43.6	57.0	67.9	45.8	56.5	60.4	44.0	43.6	67.7	63.1	51.5	74.3	56.3
DANN [4]	45.6	59.3	70.1	47.0	58.5	60.9	46.1	43.7	68.5	63.2	51.8	76.8	57.6
MCD [6]	48.9	68.3	74.6	61.3	67.6	68.8	57	47.1	75.1	69.1	52.2	79.6	64.1
SAFN [18]	52.0	71.7	76.3	64.2	69.9	71.9	63.7	51.4	77.1	70.9	57.1	81.5	67.3
Symnets [54]	47.7	72.9	78.5	64.2	71.3	74.2	64.2	48.8	79.5	74.5	52.6	82.7	67.6
MDD [55]	54.9	73.7	77.8	60.0	71.4	71.8	61.2	53.6	78.1	72.5	60.2	82.3	68.1
EntMin	43.2	68.4	78.4	61.4	69.9	71.4	58.5	44.2	78.2	71.1	47.6	81.8	64.5
BFM	43.3	69.1	78.0	61.3	67.4	70.9	57.8	44.1	78.9	72.1	50.1	81.0	64.5
BNM	52.3	73.9	80.0	63.3	72.9	74.9	61.7	49.5	79.7	70.5	53.6	82.2	67.9
FBNM	54.9	73.4	79.3	62.6	73.6	74.5	61.0	51.7	79.6	70.1	57.1	82.3	68.3
BNM ²	55.8	74.8	79.9	64.2	73.7	75.5	61.6	52.4	80.4	72.2	56.8	83.5	69.2
FBNM ²	55.3	75.4	79.9	64.0	74.2	75.5	62.2	52.0	80.4	72.3	57.0	83.4	69.3
CDAN [14]	50.7	70.6	76.0	57.6	70.0	70.0	57.4	50.9	77.3	70.9	56.7	81.6	65.8
CDAN+EntMin	54.1	72.4	78.3	61.8	71.8	73.0	62.0	52.3	79.7	72.0	57.0	83.2	68.1
CDAN+BNM	56.1	75.0	79.0	63.3	73.1	74.0	62.4	53.6	80.9	72.2	58.6	83.5	69.3
CDAN+BNM ²	55.8	75.1	79.1	63.3	73.2	74.1	62.6	53.3	80.7	72.2	59.0	83.8	69.4
CDAN+FBNM	56.3	74.6	79.3	63.4	73.2	73.9	62.7	53.5	81.0	72.7	58.7	83.6	69.4
CDAN+FBNM ²	56.1	74.9	79.3	63.6	73.6	74.1	62.9	54.1	81.0	72.5	58.4	83.6	69.5
HDAN [15]	56.8	75.2	79.8	65.1	73.9	75.2	66.3	56.7	81.8	75.4	59.7	84.7	70.9
HDAN+BNM	57.4	75.8	80.3	66.1	74.3	75.4	67.0	57.6	81.9	74.9	59.7	84.7	71.3
HDAN+BNM ²	57.3	75.8	80.3	66.1	74.7	75.8	66.7	58.0	81.9	75.1	59.9	84.7	71.4
HDAN+FBNM	57.6	75.9	80.3	65.7	74.1	75.8	66.8	57.7	82.0	74.9	59.6	84.7	71.3
HDAN+FBNM ²	57.4	75.7	80.2	66.3	74.5	75.7	67.5	57.9	81.9	75.2	59.7	84.7	71.4
SHOT [16]	57.1	78.1	81.5	68.0	78.2	78.1	67.4	54.9	82.2	73.3	58.8	84.3	71.8
FBNM-S	56.9	77.7	81.6	68.1	77.6	79.2	67.7	55.3	82.2	73.7	59.8	84.7	72.0
BNM-S	57.4	77.8	81.7	67.8	77.6	79.3	67.6	55.7	82.2	73.5	59.5	84.7	72.1

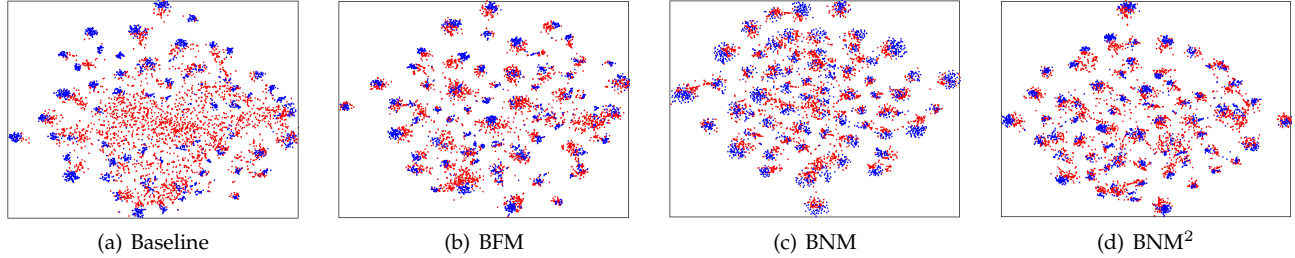


Fig. 6. Visualization results with T-SNE of different methods on Ar → Cl. The source samples are in blue and target samples in red.

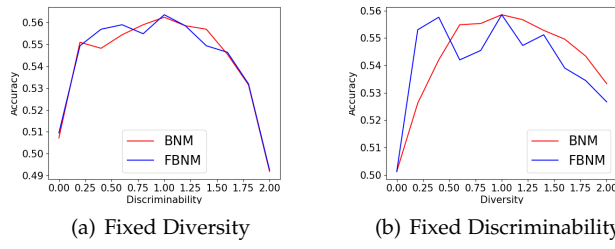


Fig. 7. Accuracy under different radio of discriminability and diversity.

by higher baseline accuracy in Ar → Pr. Thus BNM is more effective in difficult tasks with rich data near the decision boundary.

For the trade-off between improvement on prediction discriminability and diversity, we show the results with different ratios in Figure 7. Different ratios is achieved by harmonizing the results of F -norm and nuclear-norm. F -norm denotes the merely discriminability while nuclear-norm denotes both discriminability and diversity. The weight of

nuclear-norm is set to be 1, when diversity is fixed. Under fixed diversity, both BNM and FBNM could reach optimal results when discriminability is set to be 1, where the parameter of F -norm is set to be 0. Meanwhile, the sum of weights for nuclear-norm and F -norm is fixed, when discriminability is fixed. Both BNM and FBNM reaches optimal solutions when diversity is set to be 1. The results show that discriminability and diversity should be set with equal weights, which satisfies the circumstances of nuclear-

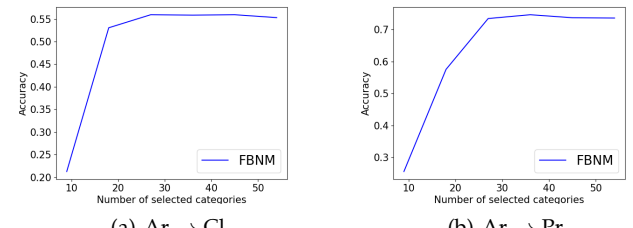


Fig. 8. Accuracy under different select categories numbers under FBNM.

TABLE 4
Accuracies (%) on Balance Domainnet of ResNet50-based UDA methods.

Methods	R→C		R→P		P→C		C→S		S→P		R→S		P→R		Avg	
	Src	Tgt														
Baseline1 [50]	84.1	67.3	84.1	70.6	73.1	59.5	77.5	62.0	71.7	58.5	84.1	64.6	73.1	71.7	78.3	64.9
Baseline2 [50]	82.8	68.1	84.3	71.9	68.9	60.7	75.5	63.0	71.3	62.7	81.8	64.9	72.5	72.6	76.7	66.3
DAN	82.1	68.3	84.0	71.8	69.4	61.4	75.8	63.8	71.7	63.5	81.3	65.1	71.6	71.9	76.6	66.6
DANN	81.2	69.3	82.6	72.7	65.0	58.5	72.5	64.1	70.1	61.9	80.5	67.8	69.0	70.2	74.4	66.4
ENT [44]	82.0	69.1	83.9	71.4	69.2	62.4	74.9	62.4	71.5	64.0	81.4	65.8	71.4	73.5	76.3	66.9
SAFN [18]	82.5	67.9	84.4	71.5	69.3	60.5	75.9	63.1	71.0	63.1	81.9	64.6	72.0	72.4	76.7	66.2
CDAN [14]	80.8	70.2	82.1	73.0	66.9	61.8	72.9	65.8	70.0	63.2	80.2	69.3	69.7	71.1	74.7	67.8
BFM	82.5	69.4	84.6	73.5	69.0	62.2	76.1	65.2	72.1	64.5	82.2	67.8	72.9	74.2	77.1	68.1
BNM($K = 1$)	82.5	69.7	84.6	73.8	68.5	62.6	76.6	65.6	72.4	65.5	81.9	67.8	73.0	74.4	77.1	68.5
BNM($K = 2$)	82.4	70.2	84.4	74.2	69.2	63.8	76.0	65.9	72.2	65.7	81.4	67.9	73.1	74.6	77.0	68.9
BNM($K = 3$)	82.4	70.5	84.4	74.2	69.3	63.4	75.9	65.8	72.2	65.6	81.3	68.1	73.1	74.7	77.0	68.9
BNM ²	82.2	70.4	83.9	73.8	68.5	63.4	76.5	65.9	71.8	65.5	81.3	67.7	71.9	74.3	76.6	68.7
FBNM	82.1	70.4	84.4	74.0	68.7	63.2	76.3	66.2	71.5	65.3	81.5	68.0	72.9	74.6	76.8	68.8
FBNM ²	82.1	70.4	84.6	74.2	68.7	63.4	75.6	65.9	72.2	65.5	81.2	67.9	72.9	74.6	76.7	68.8
HDAN [15]	82.8	72.8	84.3	74.8	70.5	65.8	75.1	68.0	71.7	66.6	82.8	71.6	73.0	75.4	77.2	70.7
HDAN+BNM	82.3	72.7	84.3	74.7	70.5	66.1	76.3	68.0	72.6	67.7	82.5	71.3	72.7	75.5	77.3	70.9
HDAN+BNM ²	82.2	72.9	84.2	75.2	69.4	65.1	75.3	67.7	71.7	66.8	82.0	71.2	72.5	75.1	76.8	70.6
HDAN+FBNM	82.6	73.2	84.5	75.4	69.4	65.1	76.0	68.5	72.0	67.0	82.3	71.6	72.7	75.6	77.1	70.9
HDAN+FBNM ²	82.4	73.0	84.3	75.0	70.0	65.8	75.5	68.2	71.2	66.5	82.1	71.4	72.8	75.6	76.9	70.8

norm.

To analyze the proper number of the selected categories for FBNM. We show the accuracy under different numbers of select categories under FBNM in Figure 8. The batch size is 36, and 36 categories are selected to approximate the nuclear-norm. While we find more or less selected categories will damage the overall accuracy for both Ar → Cl and Ar → Pr. For example, 18 selected categories hold 53.1 accuracy, with 2.7 degradation compared with 36 batch size. The results will reach optimal if the batch size is near 36.

We also visualize the T-SNE results of Ar → Cl in Figure 6, with source domain in blue and target domain in red. The visualization shows the large gap between source and target domain in Baseline method, trained only on source domain. The large domain gap is reduced by increasing prediction discriminability in BFM. In BNM, the visualization shows more red points near the blue points, with higher prediction diversity. By integrating more categories, BNM outperforms BFM on the overall accuracy in most tasks, which shows the importance of diversity. However, BNM still suffers from the problem that the samples are not tightly connected. BNM² mitigates the problem by reducing the discriminability on source domain, with less distance between blue and red points.

4.2 Balance Domainnet

To show the effect of our method, we construct Balance Domainnet where each category contains identical number of samples selected from Domainnet [20]. In Balance Domainnet, there are four domains including Real (R), Clipart (C), Painting (P) and Sketch (S) with large domain discrepancy. Each domain holds total 126 categories, with at least 50 training samples for each category. To maintain balanced for all the categories, different categories contain the same number of samples for one domain. The transfer tasks are selected by 7 domain adaptation scenarios, following [21].

TABLE 5
Comparisons on numbers of samples for categories.

Dataset	Domain	Sum	Mean	Std	Max	Min
Office-31	Amazon	2817	90.9	13.5	100	36
	Dslr	498	16.1	5.7	31	7
Office-Home	Art	2427	37.3	19.6	99	15
	Clipart	4365	67.2	24.1	99	39
Domainnet	Clipart (train)	34019	98.6	55.3	328	8
	Clipart (test)	14814	42.9	23.7	141	4
	Real (train)	122563	355.3	121.0	570	21
	Real (test)	52764	152.9	51.8	245	10
Semi	Clipart	18703	148.4	87.9	469	12
	Real	70358	558.4	142.4	804	147
Balance	Clipart (train)	6300	50	0	50	50
	Clipart (test)	2772	22	0	22	22
	Real (train)	8568	68	0	68	68
	Real (test)	3780	30	0	30	30

We also compare the number of samples in existing datasets as shown in Table 5, discussed in Supplementary in detail. We list the sum of samples (Sum), Mean category number (Mean), Standard category number (Std), Maximum category number (Max) and Minimum category number (Min). We could find that existing datasets of Office-31, Office-Home, Domainnet and Semi Domainnet contain imbalanced categories, where Std monotonically increase with Mean. Typically, in Clipart (train) of Domainnet, the largest sample number in categories is 328, while only 8 samples exist in another category. The imbalanced dataset would inevitably result in prediction bias, with improper conclusions for domain adaptation.

To explore our method under balanced circumstance, we show the results on Balance Domainnet in Table 4. Baseline1 refers to model trained with only source data, while Baseline2 refers to model trained with only source data along with updating the batch normalization (BN) [59] layer with target unlabeled data. Updating BN layer could result in performance degradation on source domain, and improve

TABLE 6

Calculation time (s per 1000 times) under different B and C .						
B Number	100	100	100	1000	10000	1000
C Number	100	1000	10000	100	100	1000
BNM	0.89	2.72	18.62	1.93	6.39	105.54
EntMin [44]	0.05	0.12	1.80	0.12	1.64	1.69
FBNM	0.05	0.11	0.82	0.08	0.30	1.49
BNM / FBNM	16.34	23.88	22.66	24.20	21.62	70.78

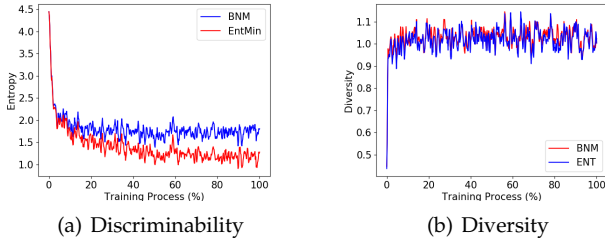


Fig. 9. Prediction discriminability and diversity for $R \rightarrow C$. Prediction discriminability is shown by entropy, while diversity is measured by average matrix rank dividing the average ground-truth category number.

the results on target domain. Directly increasing discriminability on target domain by BFM could achieve well-performed results. However, BNM could still increase the results under balanced situations compared with BFM. The results validate that promoting the prediction diversity is necessary even in a balanced dataset. Meanwhile, compared with Baseline2, BNM could achieve higher performance on source domain, which also validates the effectiveness of BNM.

Considering the large gap between batch size $B = 36$ and category number $C = 126$ in Balance Domainnet, we try different multiple number K , and we find BNM could perform well when K is 2 or 3. Thus BNM could be fully explored when multiple B is larger or a bit smaller than C . Meanwhile, BNM could still improve the performance of HDAN. However, BNM^2 does not outperform BNM under balanced dataset. The results show that the reduction of source domain does improve the performance, which means BNMin is more suitable for imbalanced small-scale source domain. The results also validate a conclusion that balanced large-scale source domain hold less concern on overfitting. In terms of the scenarios, BNM could achieve well-performed results on difficult tasks, such as $S \rightarrow P$.

Under balanced situation, the prediction discriminability and diversity are shown in Figure 9. BNM and EntMin could both increase prediction discriminability as shown in Figure 9(a). Since EntMin focuses on only discriminability, more discriminability could be achieved in EntMin. On the contrary, though with slight advantages, BNM could still increase the prediction diversity compared with EntMin as shown in Figure 9(b). In Table 4, BNM could achieve more accurate predictions compared with EntMin. The comparison shows that prediction discriminability and diversity should both be increased, even in balanced situation.

To show that the approximation could speed up the training procedure, we calculate the training time in Table 6. The results are based on Pytorch on devices of CPU Intel(R) Core(TM) i7-4790K CPU @ 4.00GHz with 4 cpu cores. We run the results by randomly generating matrix A , to calculate typical measurements, and the time generating matrix A is removed from the calculation time. We calculate the total

time of measurements on 1000 random matrix A . We denote the training time of BNM dividing FBNM as BNM/FBNM. The results show that FBNM is faster than EntMin and BNM for all situations. As an approximation method, FBNM could greatly shorten the calculation time of BNM, such as 105.54 to 1.49 in matrix with $B = 1000$, $C = 1000$. Also, we could find the gradual improvement on BNM/FBNM, from $B = 100$, $C = 100$ to $B = 1000$ and $C = 1000$. The results show that FBNM could reduce the computation complexity by approximately n , which also validate that FBNM reduces the computation complexity from $O(n^3)$ to $O(n^2)$.

4.3 Semi-supervised Domain Adaptation

Semi-supervised domain adaptation (SSDA) is a more realistic setting, where domain adaptation is performed with labeled source data to partially labeled target data. In SSDA, we utilize typical dataset of Semi Domainnet proposed in [21], which is selected from DomainNet [20]. We take the same protocol with [21] where the four domains including Real (R), Clipart (C), Painting (P) and Sketch (S) in total 126 categories. In this paper, following [21], seven domain adaptation scenarios are formulated on the four domains, showing different levels of domain gap. All the methods are evaluated under the one-shot and three-shot settings the same as [21], where there are only 1 or 3 labeled samples per category in target domain.

We use ResNet34 [50] as the backbones of the generator, optimized by SGD. The initial learning rate is 0.001, with the momentum of 0.9. BNM loss is combined with classification loss with the parameter λ fixed to 0.5. When BNM is regarded as a typical method, the source batch size is 24 and target batch size is 48, with multiple number as 1. When BNM is combined with existing methods, the source and target batch size is 24, with the multiple number as 3. For fair comparison, we run three random experiments and report the average accuracy.

The quantitative results on Semi Domainnet are summarized in Table 7. It is easily observed that BNM outperforms competitors on most settings, and achieves well performed results on average. The simple BNM method outperforms min-max entropy by a large margin, especially in difficult scenarios such as 1_{shot} and 3_{shot} $C \rightarrow S$. Meanwhile, to show the effect of BNM under SSDA, we also combine BNM with existing method of HDAN. The improvement on HDAN means that existing method might still lack of enough prediction discriminability and diversity.

Compared with the basic BNM, BNM^2 could further improve the performance on both 1 shot and 3 shot situations. Surprisingly, FBNM achieves better results compared with BNM, which shows the superiority of the approximated method. When cooperated with HDAN, BNM^2 could still slightly outperform BNM in most cases. However, in some scenarios, the training process might not converge, denoted as * on performance, such as 1_{shot} $R \rightarrow C$. The converge problem results from the complex computation of singular value decomposition, and the convergence during the decomposition procedure. Compared with original calculation of nuclear-norm, our approximated method could solve the problem of the convergence by simply combining the components.

TABLE 7
Accuracies (%) on Semi DomainNet subset of ResNet34-based SSDA methods.

Methods	R→C		R→P		P→C		C→S		S→P		R→S		P→R		Avg	
	1shot	3shot														
ResNet34 [50]	55.6	60.0	60.6	62.2	56.8	59.4	50.8	55.0	56.0	59.5	46.3	50.1	71.8	73.9	56.9	60.0
DANN [4]	58.2	59.8	61.4	62.8	56.3	59.6	52.8	55.4	57.4	59.9	52.2	54.9	70.3	72.2	58.4	60.7
ADR [58]	57.1	60.7	61.3	61.9	57.0	60.7	51.0	54.4	56.0	59.9	49.0	51.1	72.0	74.2	57.6	60.4
CDAN [14]	65.0	69.0	64.9	67.3	63.7	68.4	53.1	57.8	63.4	65.3	54.5	59.0	73.2	78.5	62.5	66.5
EntMin [44]	65.2	71.0	65.9	69.2	65.4	71.1	54.6	60.0	59.7	62.1	52.1	61.1	75.0	78.6	62.6	67.6
MME [21]	70.0	72.2	67.7	69.7	69.0	71.7	56.3	61.8	64.8	66.8	61.0	61.9	76.1	78.5	66.4	68.9
GVBG [29]	70.8	73.3	65.9	68.7	71.1	72.9	62.4	65.3	65.1	66.6	67.1	68.5	76.8	79.2	68.4	70.6
BNM	70.6	72.7	69.1	70.2	71.0	72.5	61.3	63.9	67.2	68.8	61.0	63.0	78.2	80.3	68.3	70.2
BNM ²	71.4	72.8	69.3	70.5	70.8	73.0	61.3	64.1	67.4	68.7	61.4	63.4	78.9	80.5	68.6	70.4
FBNM	71.1	72.6	69.2	70.3	70.8	72.9	61.3	64.3	67.2	68.9	61.3	63.4	78.9	80.4	68.5	70.4
FBNM ²	71.0	73.2	69.2	70.6	71.1	72.9	61.0	64.8	67.3	68.9	60.9	63.3	78.9	80.4	68.5	70.6
HDAN [15]	71.7	74.1	70.3	71.6	71.0	73.6	62.4	64.5	68.2	69.5	63.3	65.5	79.1	80.9	69.4	71.4
HDAN+BNM	72.5	74.5	70.8	71.9	71.5	74.3	63.5	64.7	68.8	70.1	63.8	66.1	80.3	81.4	70.2	71.8
HDAN+BNM ²	*	74.5	70.9	72.1	71.7	74.3	*	65.0	68.9	70.1	*	65.8	*	81.4	*	71.9
HDAN+FBNM	71.8	74.0	70.9	72.0	72.0	73.6	63.2	66.5	69.0	70.5	64.2	65.8	79.8	81.2	70.1	71.9
HDAN+FBNM ²	72.0	73.6	70.8	72.0	71.9	73.7	63.3	66.3	69.1	70.4	64.2	65.9	79.8	81.3	70.2	71.9

TABLE 8

Accuracies (%) and other measurements on I2AwA for ResNet50-based unsupervised open domain recognition methods.

Method	Discri.	Diversity	Time	Known	Unknown	All	Avg
zGCN [62]	.	.	.	77.2	21.0	65.0	49.1
dGCN [65]	.	.	.	78.2	11.6	64	44.9
adGCN [65]	.	.	.	77.3	15.0	64.1	46.2
bGCN [37]	.	.	.	84.6	28.0	72.6	56.3
pmdbGCN [66]	.	.	.	84.7	27.1	72.5	55.9
UODTN [12]	.	.	.	84.7	31.7	73.5	58.2
Balance* [12]	-0.759	0.945	1665.0	85.9	22.3	72.4	54.1
EntMin	-0.216	0.839	1786.3	87.5	7.2	70.5	47.4
BFM	-0.260	0.852	1678.3	87.7	9.2	71.1	48.4
BNM	-0.246	0.951	1768.3	88.3	39.7	78.0	64.0
BNM ²	-0.398	0.950	1779.4	85.2	49.5	77.6	67.4
FBNM	-0.314	0.969	1661.9	88.0	43.6	78.6	65.8
FBNM ²	-0.329	0.962	1663.0	87.4	49.2	79.3	68.3

4.4 Unsupervised Open Domain Recognition

For unsupervised open domain recognition, we evaluate our methods on I2AwA [12]. In I2AwA, source domain consists of 2,970 images belonging to 40 known categories, via selecting images from ImageNet and Google image search engine. Target domain of I2AwA is AwA2 [60] which contains 37,322 images in total. The target images belong to 50 categories, the same 40 known categories with source domain, and the remaining 10 individual classes as unknown categories.

To obtain reliable initial task model on unknown categories, we construct the same knowledge graph for I2AwA with UODTN [12]. The graph structure is constructed according to Graph Convolutional Networks (GCN) [61], [62]. The graph nodes include all categories of target domain along with the children and ancestors of the categories in WordNet [63]. To obtain features of the nodes, we utilize the word vectors extracted via the GloVe text model [64] trained on Wikipedia. We use ResNet50 [50] pretrained on ImageNet [56] as our backbone. The parameters of the last fully connected layer are initialized by the parameters of GCN in the same categories.

For fair comparison, we perform in the same environ-

TABLE 9

Parameter Sensitivity on the I2AwA dataset for ResNet50-based unsupervised open domain recognition methods.

Method	Discri.	Diversity	Time	Known	Unknown	All	Avg
BNM ($\lambda = 1$)	0.340	0.952	1768.4	88.0	39.4	77.7	63.7
BNM ($\lambda = 1.5$)	0.290	0.956	1770.2	88.1	39.7	77.9	63.9
BNM ($\lambda = 2$)	0.246	0.951	1768.3	88.3	39.7	78.0	64.0
BNM ($\lambda = 3$)	0.208	0.958	1772.8	87.7	39.5	77.5	63.6
BNM ($\lambda = 4$)	0.183	0.962	1767.4	87.4	38.6	77.1	63.0

ment with UODTN [12]. The experiments are implemented by Pytorch [57]. We fix the batch size to 48 for both source and target domain. To train the network, we apply BNM on the classification outputs on the total 50 categories for target domain, and minimize classification loss on the known 40 categories in source domain. Parameter λ is set to be 2 for BNM, FBNM and FBNM², while 1 for BNM². We report the prediction results of known categories, unknown categories, all target categories, the average of known and unknown category accuracy, along with the measurements of prediction discriminability and diversity. The prediction discriminability (denoted as Discri. in short) is measured by negative entropy to ensure more discriminability with larger negative entropy. While prediction diversity is measured by average predicted matrix rank dividing average ground truth matrix rank. To show the superiority of approximation, we also calculate the training time for 6000 iterations on device of GeForce RTX 3090, denoted as Time. For each method, we run four random experiments and report the average result.

The results are shown in Table 9, we achieve remarkable improvement on I2AwA. From the view of prediction accuracy, we achieve 11.4% improvement on the known categories compared with the baseline zGCN, and BNM surprisingly improves by 19.0% on the unknown categories over zGCN. From the overall range of the dataset, we achieve 13.3% improvement on the whole dataset and we achieve an average improvement of 15.2% improvement over zGCN. Besides, BNM outperforms the state-of-the-art

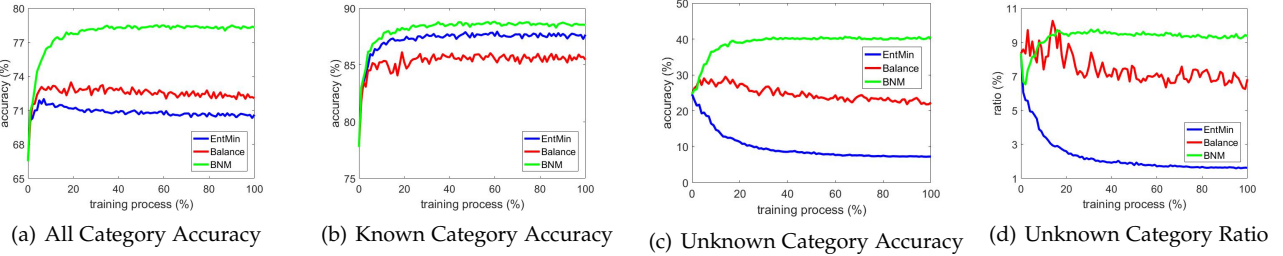


Fig. 10. Statistics for Entropy, Balance and Nuclear-norm in the whole training process for unsupervised open domain recognition.

UODTN [12] by 4.8%. The results show that the simple BNM is effective enough for unsupervised open domain recognition, which outperforms the combination of complex functions in UODTN. Besides, compared with BNM, BNM² could achieve higher average accuracy of known and unknown categories by promoting more accurate predictions on unknown categories. Surprisingly, the approximated methods of FBNM and FBNM² could achieve more accurate predictions on all sample accuracy and average category predictions, compared with BNM and BNM². Among our methods, FBNM² achieves best results on both accuracy of All and Avg, with 10.1% improvement on Avg and 5.8% improvement on all compared with UODTN.

Also, BNM could improve typical measurements of discriminability and diversity. Compared with Balance, BNM could improve the prediction discriminability from -0.759 to -0.246 . Though EntMin could ensure prediction discriminability, excessively increasing discriminability seems to be unsatisfying. In terms of prediction diversity, the diversity ratio is improved from 0.839 in EntMin to 0.969 in BNM. We also find that the approximation method could achieve better prediction results by ensuring more prediction diversity. From BNM to FBNM, diversity ratio changes from 0.951 to 0.969, with all accuracy from 78.0 to 78.6 and average accuracy from 64.0 to 65.8. In terms of the training time, the approximated methods hold the advantages of the training time, with reduction from 1768.3 to 1661.9 seconds by replacing BNM to FBNM.

We show the parameter sensitivity experiments in Table 9. The results show BNM is relatively stable under different λ , such as the training time, known category accuracy and all accuracy. In terms of λ , the performance of all and avg reaches the highest when λ equals 2. As for the transfer properties, larger λ means relatively more prediction discriminability and diversity for target domain. Excessive prediction discriminability and diversity could reduce the knowledge learned by source domain. Thus proper value of λ is also important for the methods, and we set λ fixed to 2 for further comparison.

We also compare the training process of EntMin, Balance and BNM loss functions in Figure 10. The prediction results on all categories, known categories and unknown categories are separately shown in Figure 10(a), 10(b) and 10(c). BNM outperforms competitors on all accuracy, known category accuracy and unknown category accuracy in the whole training process. To explore the intrinsic effect of BNM on unknown categories, we show the unknown category ratio, which is the ratio of predicting the samples in target domain of I2AwA into unknown categories in Figure 10(d).

Obviously, EntMin reduces the unknown category ratio by a large margin, which greatly damages the prediction diversity and accuracy on unknown categories. Though the unknown category ratio in BNM is reduced at first, it gradually raises along the training process, and it appears to be even higher than initial ratio after training. This means BNM could increase prediction diversity by ensuring ratio of predictions on minority categories. Though the Balance constraint could also protect ratio of prediction on minority categories, results of Balance loss seem not to be stable. Besides, the accuracy of Balance loss is much lower than BNM due to the lack of discriminability. The experimental phenomenon has steadily proved the effectiveness of BNM towards both discriminability and diversity.

4.5 Discussion

The chosen tasks are typical domain adaptation circumstances to show the effect of BNM. Among the tasks and datasets, there are mainly differences in three aspects, *i.e.*, the domain discrepancy, category imbalance ratio and category number. There exists less domain discrepancy for Office-31, while large domain discrepancy for other datasets. From the balance view, the categories are only balanced in Balance Domainnet of UDA. While in Office-31 and Office-Home of UDA and semi-Domainnet of SSDA, the categories are imbalanced. Meanwhile, I2AwA of UODR is a task with extremely imbalanced category distributions, where some categories are even unseen in source domain. In terms of the category number, the category number is relative small in Office-31, Office-Home and I2AwA, while relative large in Semi Domainnet and Balance Domainnet.

In terms of domain discrepancy, BNM performs well in most cases. Thus BNM is suitable for both large and small domain discrepancy, while experiments show that BNM could obviously improve the results when large domain discrepancy exists. In terms of the imbalance ratio, BNM can perform well on strictly balanced dataset of Balance Domainnet, and also other imbalanced domain adaptation scenarios. Therefore, in both imbalanced and balanced situations, maintaining prediction diversity by BNM is necessary. In UODR, the simple BNM even achieves state-of-the-art results, thus BNM will perform better under imbalanced situations.

For the variants of BNM, BNM² outperforms BNM in most cases, except Balance Domainnet. The differences between BNM² and BNM lie in BNMin, thus BNMin will perform under imbalanced small-scale circumstance. In BNM, batch size should not be negligible small compared with

category number. In Office-31, Office-Home and I2AwA the category number is similar to the batch size, and BNM performs well. While in Balance Domainnet and Semi Domainnet, we are required to enlarge the batch size by multiple batch optimization. Meanwhile, the fast method FBNM could achieve similar results compared with BNM in all the tasks, and the applicability of FBNM (FBNM²) is the same with BNM (BNM²).

5 CONCLUSION

Prediction discriminability and diversity could be separately measured by the Frobenius-norm and rank of the batch output matrix. Nuclear-norm is the upperbound of Frobenius-norm, and also the convex approximation of matrix rank. Accordingly, we propose BNM method which maximizes the batch nuclear-norm to ensure higher prediction discriminability and diversity on target domain. Meanwhile, we minimize the nuclear-norm on source output matrix for reliable knowledge transfer. We also propose an approximation of nuclear norm to speed up the training procedure. Experiments show our methods are suitable for three domain adaptation scenarios.

Acknowledgement. This work was supported in part by the National Key R&D Program of China under Grant 2018AAA0102003, in part by National Natural Science Foundation of China: 61672497, 61620106009, 61836002, 61931008, 61771457, 61732007 and U1636214, and in part by Key Research Program of Frontier Sciences, CAS: QYZDJ-SSW-SYS013.

REFERENCES

- [1] M. Long, Y. Cao, J. Wang, and M. I. Jordan, "Learning transferable features with deep adaptation networks," in *Proceedings of the 32nd International Conference on Machine Learning, ICML 2015, Lille, France, 6-11 July 2015*, 2015, pp. 97–105.
- [2] B. Sun and K. Saenko, "Deep coral: Correlation alignment for deep domain adaptation," in *European Conference on Computer Vision*. Springer, 2016, pp. 443–450.
- [3] H. Yan, Y. Ding, P. Li, Q. Wang, Y. Xu, and W. Zuo, "Mind the class weight bias: Weighted maximum mean discrepancy for unsupervised domain adaptation," in *Proceedings of the IEEE Conference on Computer Vision and Pattern Recognition*, 2017, pp. 2272–2281.
- [4] Y. Ganin, E. Ustinova, H. Ajakan, P. Germain, H. Larochelle, F. Laviolette, M. Marchand, and V. Lempitsky, "Domain-adversarial training of neural networks," *The Journal of Machine Learning Research*, vol. 17, no. 1, pp. 2096–2030, 2016.
- [5] J. Hoffman, E. Tzeng, T. Park, J.-Y. Zhu, P. Isola, K. Saenko, A. A. Efros, and T. Darrell, "Cycada: Cycle-consistent adversarial domain adaptation," *arXiv preprint arXiv:1711.03213*, 2017.
- [6] K. Saito, K. Watanabe, Y. Ushiku, and T. Harada, "Maximum classifier discrepancy for unsupervised domain adaptation," in *Proceedings of the IEEE Conference on Computer Vision and Pattern Recognition*, 2018, pp. 3723–3732.
- [7] M. Long, H. Zhu, J. Wang, and M. I. Jordan, "Unsupervised domain adaptation with residual transfer networks," in *NIPS*, 2016, pp. 136–144. [Online]. Available: <http://papers.nips.cc/paper/6110-unsupervised-domain-adaptation-with-residual-transfer-networks.pdf>
- [8] T.-H. Vu, H. Jain, M. Bucher, M. Cord, and P. Pérez, "Advent: Adversarial entropy minimization for domain adaptation in semantic segmentation," in *Proceedings of the IEEE Conference on Computer Vision and Pattern Recognition*, 2019, pp. 2517–2526.
- [9] Y. Zou, Z. Yu, B. Vijaya Kumar, and J. Wang, "Unsupervised domain adaptation for semantic segmentation via class-balanced self-training," in *Proceedings of the European conference on computer vision (ECCV)*, 2018, pp. 289–305.
- [10] Y. Zou, Z. Yu, X. Liu, B. Kumar, and J. Wang, "Confidence regularized self-training," in *Proceedings of the IEEE International Conference on Computer Vision*, 2019, pp. 5982–5991.
- [11] C. E. Shannon, "A mathematical theory of communication," *Bell system technical journal*, vol. 27, no. 3, pp. 379–423, 1948.
- [12] J. Zhuo, S. Wang, S. Cui, and Q. Huang, "Unsupervised open domain recognition by semantic discrepancy minimization," in *Proceedings of the IEEE Conference on Computer Vision and Pattern Recognition*, 2019, pp. 750–759.
- [13] S. Cui, S. Wang, J. Zhuo, L. Li, Q. Huang, and Q. Tian, "Towards discriminability and diversity: Batch nuclear-norm maximization under label insufficient situations," in *IEEE/CVF Conference on Computer Vision and Pattern Recognition (CVPR)*, June 2020.
- [14] M. Long, Z. Cao, J. Wang, and M. I. Jordan, "Conditional adversarial domain adaptation," in *Advances in Neural Information Processing Systems*, 2018, pp. 1647–1657.
- [15] S. Cui, X. Jin, S. Wang, Y. He, and Q. Huang, "Heuristic domain adaptation," in *Advances in Neural Information Processing Systems*, 2020.
- [16] J. Liang, D. Hu, and J. Feng, "Do we really need to access the source data? source hypothesis transfer for unsupervised domain adaptation," in *International Conference on Machine Learning*. PMLR, 2020, pp. 6028–6039.
- [17] K. Saenko, B. Kulis, M. Fritz, and T. Darrell, "Adapting visual category models to new domains," in *European conference on computer vision*. Springer, 2010, pp. 213–226.
- [18] R. Xu, G. Li, J. Yang, and L. Lin, "Larger norm more transferable: An adaptive feature norm approach for unsupervised domain adaptation," in *The IEEE International Conference on Computer Vision (ICCV)*, October 2019.
- [19] R. Xu, Z. Chen, W. Zuo, J. Yan, and L. Lin, "Deep cocktail network: Multi-source unsupervised domain adaptation with category shift," in *The IEEE Conference on Computer Vision and Pattern Recognition (CVPR)*, June 2018.
- [20] X. Peng, Q. Bai, X. Xia, Z. Huang, K. Saenko, and B. Wang, "Moment matching for multi-source domain adaptation," in *Proceedings of the IEEE International Conference on Computer Vision*, 2019, pp. 1406–1415.
- [21] K. Saito, D. Kim, S. Sclaroff, T. Darrell, and K. Saenko, "Semi-supervised domain adaptation via minimax entropy," in *Proceedings of the IEEE International Conference on Computer Vision*, 2019, pp. 8050–8058.
- [22] Y. Jin, X. Wang, M. Long, and J. Wang, "Minimum class confusion for versatile domain adaptation," in *Proceedings of the European conference on computer vision (ECCV)*, 2020, pp. 464–480.
- [23] A. Gretton, K. M. Borgwardt, M. J. Rasch, B. Schölkopf, and A. Smola, "A kernel two-sample test," *Journal of Machine Learning Research*, vol. 13, no. Mar, pp. 723–773, 2012.
- [24] M. Long, H. Zhu, J. Wang, and M. I. Jordan, "Deep transfer learning with joint adaptation networks," in *Proceedings of the 34th International Conference on Machine Learning-Volume 70*. JMLR.org, 2017, pp. 2208–2217.
- [25] J. Zhuo, S. Wang, W. Zhang, and Q. Huang, "Deep unsupervised convolutional domain adaptation," in *Proceedings of the 25th ACM international conference on Multimedia*. ACM, 2017, pp. 261–269.
- [26] G. Kang, L. Zheng, Y. Yan, and Y. Yang, "Deep adversarial attention alignment for unsupervised domain adaptation: the benefit of target expectation maximization," in *Proceedings of the European Conference on Computer Vision (ECCV)*, 2018, pp. 401–416.
- [27] I. Goodfellow, J. Pouget-Abadie, M. Mirza, B. Xu, D. Warde-Farley, S. Ozair, A. Courville, and Y. Bengio, "Generative adversarial nets," in *Advances in neural information processing systems*, 2014, pp. 2672–2680.
- [28] E. Tzeng, J. Hoffman, K. Saenko, and T. Darrell, "Adversarial discriminative domain adaptation," in *Proceedings of the IEEE Conference on Computer Vision and Pattern Recognition*, 2017, pp. 7167–7176.
- [29] S. Cui, S. Wang, J. Zhuo, C. Su, Q. Huang, and T. Qi, "Gradually vanishing bridge for adversarial domain adaptation," in *Proceedings of the IEEE Conference on Computer Vision and Pattern Recognition*, 2020.
- [30] Y. Zou, Z. Yu, X. Liu, B. V. Kumar, and J. Wang, "Confidence regularized self-training," in *The IEEE International Conference on Computer Vision (ICCV)*, October 2019.
- [31] Z. Qi, S. Wang, C. Su, L. Su, Q. Huang, and Q. Tian, "Self-regulated learning for egocentric video activity anticipation," *IEEE*

Transactions on Pattern Analysis & Machine Intelligence, no. 01, pp. 1–1, 2021.

[32] M. Chen, H. Xue, and D. Cai, “Domain adaptation for semantic segmentation with maximum squares loss,” in *Proceedings of the IEEE International Conference on Computer Vision*, 2019, pp. 2090–2099.

[33] L. Hu, M. Kan, S. Shan, and X. Chen, “Duplex generative adversarial network for unsupervised domain adaptation,” in *Proceedings of the IEEE Conference on Computer Vision and Pattern Recognition*, 2018, pp. 1498–1507.

[34] X. Chen, S. Wang, M. Long, and J. Wang, “Transferability vs. discriminability: Batch spectral penalization for adversarial domain adaptation,” in *International Conference on Machine Learning*, 2019, pp. 1081–1090.

[35] R. Müller, S. Kornblith, and G. Hinton, “When does label smoothing help?”

[36] H. He and E. A. Garcia, “Learning from imbalanced data,” *IEEE Transactions on knowledge and data engineering*, vol. 21, no. 9, pp. 1263–1284, 2009.

[37] J. Song, C. Shen, Y. Yang, Y. Liu, and M. Song, “Transductive unbiased embedding for zero-shot learning,” in *ICCV*, 2018, pp. 1024–1033.

[38] A. Kulesza, B. Taskar *et al.*, “Determinantal point processes for machine learning,” *Foundations and Trends® in Machine Learning*, vol. 5, no. 2–3, pp. 123–286, 2012.

[39] M. Arjovsky, S. Chintala, and L. Bottou, “Wasserstein generative adversarial networks,” in *International Conference on Machine Learning*, 2017, pp. 214–223.

[40] E. J. Candès and B. Recht, “Exact matrix completion via convex optimization,” *Foundations of Computational mathematics*, vol. 9, no. 6, p. 717, 2009.

[41] J.-F. Cai, E. J. Candès, and Z. Shen, “A singular value thresholding algorithm for matrix completion,” *SIAM Journal on optimization*, vol. 20, no. 4, pp. 1956–1982, 2010.

[42] S. Gu, L. Zhang, W. Zuo, and X. Feng, “Weighted nuclear norm minimization with application to image denoising,” in *Proceedings of the IEEE conference on computer vision and pattern recognition*, 2014, pp. 2862–2869.

[43] W. Dong, G. Shi, and X. Li, “Nonlocal image restoration with bilateral variance estimation: a low-rank approach,” *IEEE transactions on image processing*, vol. 22, no. 2, pp. 700–711, 2012.

[44] Y. Grandvalet and Y. Bengio, “Semi-supervised learning by entropy minimization,” in *Advances in neural information processing systems*, 2005, pp. 529–536.

[45] M. Fazel, “Matrix rank minimization with applications,” 2002.

[46] B. Recht, M. Fazel, and P. A. Parrilo, “Guaranteed minimum-rank solutions of linear matrix equations via nuclear norm minimization,” *SIAM review*, vol. 52, no. 3, pp. 471–501, 2010.

[47] N. Srebro, J. Rennie, and T. S. Jaakkola, “Maximum-margin matrix factorization,” in *Advances in neural information processing systems*, 2005, pp. 1329–1336.

[48] T. Papadopoulou and M. I. Lourakis, “Estimating the jacobian of the singular value decomposition: Theory and applications,” in *European Conference on Computer Vision*. Springer, 2000, pp. 554–570.

[49] H. Venkateswara, J. Eusebio, S. Chakraborty, and S. Panchanathan, “Deep hashing network for unsupervised domain adaptation,” in *Proceedings of the IEEE Conference on Computer Vision and Pattern Recognition*, 2017, pp. 5018–5027.

[50] K. He, X. Zhang, S. Ren, and J. Sun, “Deep residual learning for image recognition,” in *Proceedings of the IEEE conference on computer vision and pattern recognition*, 2016, pp. 770–778.

[51] B. Gong, Y. Shi, F. Sha, and K. Grauman, “Geodesic flow kernel for unsupervised domain adaptation,” in *2012 IEEE Conference on Computer Vision and Pattern Recognition*. IEEE, 2012, pp. 2066–2073.

[52] P. O. Pinheiro, “Unsupervised domain adaptation with similarity learning,” in *Proceedings of the IEEE Conference on Computer Vision and Pattern Recognition*, 2018, pp. 8004–8013.

[53] S. Sankaranarayanan, Y. Balaji, C. D. Castillo, and R. Chellappa, “Generate to adapt: Aligning domains using generative adversarial networks,” in *Proceedings of the IEEE Conference on Computer Vision and Pattern Recognition*, 2018, pp. 8503–8512.

[54] Y. Zhang, H. Tang, K. Jia, and M. Tan, “Domain-symmetric networks for adversarial domain adaptation,” in *Proceedings of the IEEE Conference on Computer Vision and Pattern Recognition*, 2019, pp. 5031–5040.

[55] Y. Zhang, T. Liu, M. Long, and M. Jordan, “Bridging theory and algorithm for domain adaptation,” in *International Conference on Machine Learning*, 2019, pp. 7404–7413.

[56] J. Deng, W. Dong, R. Socher, L.-J. Li, K. Li, and L. Fei-Fei, “Imagenet: A large-scale hierarchical image database,” 2009.

[57] A. Paszke, S. Gross, S. Chintala, G. Chanan, E. Yang, Z. DeVito, Z. Lin, A. Desmaison, L. Antiga, and A. Lerer, “Automatic differentiation in pytorch,” 2017.

[58] K. Saito, Y. Ushiku, T. Harada, and K. Saenko, “Adversarial dropout regularization,” *arXiv preprint arXiv:1711.01575*, 2017.

[59] S. Ioffe and C. Szegedy, “Batch normalization: Accelerating deep network training by reducing internal covariate shift,” in *International conference on machine learning*. PMLR, 2015, pp. 448–456.

[60] Y. Xian, B. Schiele, and Z. Akata, “Zero-shot learning—the good, the bad and the ugly,” *arXiv preprint arXiv:1703.04394*, 2017.

[61] T. N. Kipf and M. Welling, “Semi-supervised classification with graph convolutional networks,” *arXiv preprint arXiv:1609.02907*, 2016.

[62] X. Wang, Y. Ye, and A. Gupta, “Zero-shot recognition via semantic embeddings and knowledge graphs,” in *CVPR*, 2018, pp. 6857–6866.

[63] G. A. Miller, “Wordnet: a lexical database for english,” *Communications of the ACM*, vol. 38, no. 11, pp. 39–41, 1995.

[64] J. Pennington, R. Socher, and C. Manning, “Glove: Global vectors for word representation,” in *Conference on Empirical Methods in Natural Language Processing*, 2014, pp. 1532–1543.

[65] M. Kampffmeyer, Y. Chen, X. Liang, H. Wang, Y. Zhang, and E. P. Xing, “Rethinking knowledge graph propagation for zero-shot learning,” *arXiv preprint arXiv:1805.11724*, 2018.

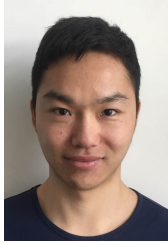
[66] J. Chen, C. Li, Y. Ru, and J. Zhu, “Population matching discrepancy and applications in deep learning,” in *NIPS*, I. Guyon, U. V. Luxburg, S. Bengio, H. Wallach, R. Fergus, S. Vishwanathan, and R. Garnett, Eds. Curran Associates, Inc., 2017, pp. 6262–6272. [Online]. Available: <http://papers.nips.cc/paper/7206-population-matching-discrepancy-and-applications-in-deep-learning.pdf>



Shuhao Cui received the B.S. degree in department of automation from Tsinghua University, Beijing, China, in 2018. He is currently pursuing the M.S. degree in the Institute of Computing Technology, Chinese Academy of Sciences. His current research interests include machine learning, computer vision and transfer learning.



Shuhui Wang received the B.S. degree in electronics engineering from Tsinghua University, Beijing, China, in 2006, and the Ph.D. degree from the Institute of Computing Technology, Chinese Academy of Sciences, Beijing, China, in 2012. He is currently a Full Professor with the Institute of Computing Technology, Chinese Academy of Sciences. He is also with the Key Laboratory of Intelligent Information Processing, Chinese Academy of Sciences. His research interests include image/video understanding/retrieval, cross-media analysis and visual-textual knowledge extraction.



Junbao Zhuo received the B.S. degree in computer science from South China University of Technology, Guangzhou, China, in 2014, and the Ph.D. degree from the Institute of Computing Technology, Chinese Academy of Sciences, Beijing, China, in 2020. He is currently a postdoctoral researcher with the Institute of Computing Technology, Chinese Academy of Sciences. He is currently a Postdoctoral Research Associate with the Institute of Computing Technology, Chinese Academy of Sciences, working with Qingming Huang. His current research interests include machine learning, deep learning and transfer learning.



Qi Tian is currently a Chief Scientist in Artificial Intelligence at Cloud BU, Huawei. From 2018-2020, he was the Chief Scientist in Computer Vision at Huawei Noah's Ark Lab. He was also a Full Professor in the Department of Computer Science, the University of Texas at San Antonio (UTSA) from 2002 to 2019. During 2008-2009, he took one-year Faculty Leave at Microsoft Research Asia (MSRA). Dr. Tian received his Ph.D. in ECE from University of Illinois at Urbana-Champaign (UIUC) and received his B.E. in

Electronic Engineering from Tsinghua University and M.S. in ECE from Drexel University, respectively. Dr. Tian's research interests include computer vision, multimedia information retrieval and machine learning and published 590+ refereed journal and conference papers. His Google citation is over 26100+ with H-index 78. He was the co-author of best papers including IEEE ICME 2019, ACM CIKM 2018, ACM ICMR 2015, PCM 2013, MMM 2013, ACM ICIMCS 2012, a Top 10% Paper Award in MMSP 2011, a Student Contest Paper in ICASSP 2006, and co-author of a Best Paper/Student Paper Candidate in ACM Multimedia 2019, ICME 2015 and PCM 2007. Dr. Tian research projects are funded by ARO, NSF, DHS, Google, FXPAL, NEC, SALS, CIAS, Akiira Media Systems, HP, Blippar and UTSA. He received 2017 UTSA President's Distinguished Award for Research Achievement, 2016 UTSA Innovation Award, 2014 Research Achievement Awards from College of Science, UTSA, 2010 Google Faculty Award, and 2010 ACM Service Award. He is the associate editor of IEEE TMM, IEEE TCSVT, ACM TOMM, MMSJ, and in the Editorial Board of Journal of Multimedia (JMM) and Journal of MVA. Dr. Tian is the Guest Editor of IEEE TMM, Journal of CVIU, etc. Dr. Tian is a Fellow of IEEE.



Liang Li received his B.S. degree from Xi'an Jiaotong University in 2008, and Ph.D. degree from Institute of Computing Technology, Chinese Academy of Sciences, Beijing, China in 2013. From 2013 to 2015, he held a post-doc position with the Department of Computer and Control Engineering, University of Chinese Academy of Sciences, Beijing, China. Currently he is serving as the associate professor at Institute of Computing Technology, Chinese Academy of Sciences. He has also served on a number of committees of international journals and conferences. Dr. Li has published over 60 refereed journal/conference papers. His research interests include multimedia content analysis, computer vision, and pattern recognition.



Qingming Huang received the B.S. degree in computer science and Ph.D. degree in computer engineering from the Harbin Institute of Technology, Harbin, China, in 1988 and 1994, respectively. He is currently a Chair Professor with the School of Computer Science and Technology, University of Chinese Academy of Sciences. He has authored over 400 academic papers in international journals, such as IEEE Transactions on Pattern Analysis and Machine Intelligence, IEEE Transactions on Image Processing, IEEE Transactions on Multimedia, IEEE Transactions on Circuits and Systems for Video Technology, and top level international conferences, including the ACM Multimedia, ICCV, CVPR, ECCV, VLDB, and IJCAI. He is the Associate Editor of IEEE Transactions on Circuits and Systems for Video Technology and the Associate Editor of Acta Automatica Sinica. His research interests include multimedia computing, image/video processing, pattern recognition, and computer vision.

Discriminability and Diversity for Domain Adaptation

1 METHOD

1.1 Monotonicity of F -norm and Entropy

To prove strict opposite monotonicity between F -norm and entropy, we separately analyze the monotonicity and the bounds between F -norm and entropy.

The F -norm of matrix A is the square root sum of all the elements in A . The calculation process could be divided into two processes, we could first calculate the quadratic sum of each row in A and then calculated the square root of sum of all the rows. Besides the condition that the monotonicity of square root of sum of all the rows depends on the monotonicity of each row, since there is no extra constraint on different rows. Thus we could simply consider the monotonicity of quadratic sum of each row to analyze the monotonicity of the F -norm on matrix. Similar for the entropy, we could also simply analyze the monotonicity of each row.

We take A_i the row i for example, and denote the square sum of row i as $f(A_i)$, thus $f(A_i)$ could be calculated as:

$$f(A_i) = \sum_{j=1}^C A_{ij}^2. \quad (1)$$

To analyze the monotonicity of a function of several input variables, we could analyze the monotonicity of the function on each variable. It should be noted that $\sum_{j=1}^C A_{ij} = 1$. Actually the variables are supposed to be independent, but to satisfy the constraint of the sum 1, we assume the variable A_{iC} is the only variable dependent on A_{ij} . Thus the partial derivative of $f(A_i)$ could be calculated as:

$$\begin{aligned} \frac{\partial f(A_i)}{\partial A_{ij}} &= 2A_{ij} - 2A_{iC} \\ &= 4A_{ij} - 2\left(1 - \sum_{k=1, k \neq j}^{C-1} A_{ik}\right), \end{aligned} \quad (2)$$

where $f(A_i)$ reaches the bound when $A_{ij} = \frac{1}{2} - \frac{1}{2} \sum_{k=1, k \neq j}^{C-1} A_{ik}$. When $A_{ij} \leq \frac{1}{2} - \frac{1}{2} \sum_{k=1, k \neq j}^{C-1} A_{ik}$ and $\frac{\partial f(A_i)}{\partial A_{ij}} \leq 0$, $f(A_i)$ will monotonously decrease. When $A_{ij} \geq \frac{1}{2} - \frac{1}{2} \sum_{k=1, k \neq j}^{C-1} A_{ik}$ and $\frac{\partial f(A_i)}{\partial A_{ij}} \geq 0$, $f(A_i)$ will monotonously increase.

For the entropy, we denote the entropy of row i as $H(A_i)$, and $H(A_i)$ could be calculated as follows:

$$H(A_i) = -\sum_{j=1}^C A_{ij} \log(A_{ij}). \quad (3)$$

Similarly, the partial derivative of $H(A_i)$ could be calculated as:

$$\begin{aligned} \frac{\partial H(A_i)}{\partial A_{ij}} &= -\log(A_{ij}) + \log(A_{iC}) \\ &= \log\left(\frac{1 - A_{ij} - \sum_{k=1, k \neq j}^{C-1} A_{ik}}{A_{ij}}\right) \end{aligned} \quad (4)$$

where $H(A_i)$ reaches the bound when $A_{ij} = \frac{1}{2} - \frac{1}{2} \sum_{k=1, k \neq j}^{C-1} A_{ik}$. When $A_{ij} \leq \frac{1}{2} - \frac{1}{2} \sum_{k=1, k \neq j}^{C-1} A_{ik}$ and $\frac{\partial H(A_i)}{\partial A_{ij}} \geq 0$, $H(A_i)$ will monotonously increase. When $A_{ij} \geq \frac{1}{2} - \frac{1}{2} \sum_{k=1, k \neq j}^{C-1} A_{ik}$ and $\frac{\partial H(A_i)}{\partial A_{ij}} \leq 0$, $H(A_i)$ will monotonously decrease. This validates that the F -norm and entropy of matrix $f(A_i)$ have strict opposite monotonicity.

1.2 F -norm

Frobenius-norm (F -norm) $\|A\|_F$ is defined as follows:

$$\|A\|_F = \sqrt{\sum_{i=1}^B \sum_{j=1}^C |A_{ij}|^2}. \quad (5)$$

We denote \times as the matrix multiplication and the trace of matrix $A \times A^\top$ is as follows:

$$\begin{aligned} \text{trace}(A \times A^\top) &= \sum_{i=1}^B \sum_{j=1}^C A_{ij} \cdot A_{i,j} \\ &= (\|A\|_F)^2 \end{aligned} \quad (6)$$

The trace of $A \times A^\top$ equals to the sum of eigenvalues of $A \times A^\top$. While the calculated eigenvalues of $A \times A^\top$ are the square of singular value of A . We denote the i th largest singular value as σ_i . Thus $\text{trace}(A \times A^\top)$ becomes quadratic sum of singular values of matrix A :

$$\text{trace}(A \times A^\top) = \sum_{i=1}^D \sigma_i^2. \quad (7)$$

Combining Eqn. 6 and 7, we could find that:

$$(\|A\|_F) = \sqrt{\sum_{i=1}^D \sigma_i^2}, \quad (8)$$

where the number of the singular values is denoted as D and $D = \text{Min}(B, C)$.

1.3 Relationship between Nuclear-norm and F -norm

We reanalyze the relation between $\|A\|_*$ and $\|A\|_F$. For the matrix A , the calculation of the nuclear-norm could be achieved by the sum of singular values of A . Thus the nuclear-norm could be calculated as follows:

$$\|A\|_* = \sum_{i=1}^D \sigma_i, \quad (9)$$

Thus we could find the upper-bound of $\|A\|_*$ as:

$$\|A\|_* = \sqrt{\left(\sum_{i=1}^D \sigma_i\right)^2} \leq \sqrt{D \cdot \sum_{i=1}^D \sigma_i^2} = \sqrt{D} \cdot \|A\|_F, \quad (10)$$

where if $\|A\|_* = \sqrt{D} \cdot \|A\|_F$, all the singular values will be the same. Similarly, we could obtain the lower-bound of $\|A\|_*$ as:

$$\|A\|_* = \sqrt{\left(\sum_{i=1}^D \sigma_i\right)^2} \geq \sqrt{\sum_{i=1}^D \sigma_i^2} = \|A\|_F, \quad (11)$$

Combining Eqn. 10 and 11, we could summarize the relationship as follows:

$$\frac{1}{\sqrt{D}} \|A\|_* \leq \|A\|_F \leq \|A\|_* \leq \sqrt{D} \cdot \|A\|_F. \quad (12)$$

Thus $\|A\|_*$ and $\|A\|_F$ could bound each other.

1.4 Approximation of Nuclear-norm

When $\|A\|_F$ is \sqrt{B} , the matrix satisfies the highest prediction discriminability. Then all the values in A are either 1 or 0, as follows:

$$A = \begin{bmatrix} 0 & 1 & 0 & \dots & 0 & 0 & 0 \\ 1 & 0 & 0 & \dots & 0 & 0 & 0 \\ 1 & 0 & 0 & \dots & 0 & 0 & 0 \\ \dots & \dots & \dots & \dots & \dots & \dots & \dots \\ 0 & 0 & 0 & \dots & 0 & 0 & 1 \\ 0 & 0 & 0 & \dots & 0 & 0 & 1 \\ 0 & 0 & 0 & \dots & 0 & 1 & 0 \end{bmatrix}. \quad (13)$$

While we could manually change the order of the samples to achieve ordered values predicting to category 1st to C th, as follows:

$$A = \begin{bmatrix} 1 & 0 & 0 & \dots & 0 & 0 & 0 \\ 1 & 0 & 0 & \dots & 0 & 0 & 0 \\ 0 & 1 & 0 & \dots & 0 & 0 & 0 \\ \dots & \dots & \dots & \dots & \dots & \dots & \dots \\ 0 & 0 & 0 & \dots & 0 & 1 & 0 \\ 0 & 0 & 0 & \dots & 0 & 0 & 1 \\ 0 & 0 & 0 & \dots & 0 & 0 & 1 \end{bmatrix}. \quad (14)$$

We find the matrix multiplication of A could be achieved by considering only the 1 values. Then we could calculate the results of matrix multiplication of A as follows:

$$A^\top \times A = \begin{bmatrix} \sum_{i=1}^B A_{i,1}^2 & 0 & 0 & 0 & 0 & 0 \\ 0 & \sum_{i=1}^B A_{i,2}^2 & 0 & 0 & 0 & 0 \\ 0 & 0 & \sum_{i=1}^B A_{i,3}^2 & 0 & 0 & 0 \\ \dots & \dots & \dots & \dots & \dots & \dots \\ 0 & 0 & 0 & \sum_{i=1}^B A_{i,C-2}^2 & 0 & 0 \\ 0 & 0 & 0 & 0 & \sum_{i=1}^B A_{i,C-1}^2 & 0 \\ 0 & 0 & 0 & 0 & 0 & \sum_{i=1}^B A_{i,C}^2 \end{bmatrix} \quad (15)$$

Though the equation, we could find $A^\top \times A$ is diagonal matrix. Then the diagonal values are the eigenvalue of matrix A . The responses of different categories are linear independent. Then the responses of category j constitute singular value of σ_{n_j} , as follows:

$$\sigma_{n_j}^2 = \sum_{i=1}^B A_{i,j}^2. \quad (16)$$

where n_j means the number of singular value constructed by category j . Meanwhile, the singular values are ordered by the specific number values. Then the j th singular value consists of the top j responses, as follows:

$$\sigma_j = \text{top}\left(\sqrt{\sum_{i=1}^B A_{i,j}^2}, j\right) \quad \forall j \in 0, \dots, D. \quad (17)$$

when $\|A\|_F$ equals \sqrt{B} .

Then when $\|A\|_F$ is near \sqrt{B} , the changes of the singular values are little. Then the j th biggest singular value σ_i could be approximated by:

$$\sigma_j \approx \text{top}\left(\sqrt{\sum_{i=1}^B A_{i,j}^2}, j\right) \quad \forall j \in 0, \dots, D. \quad (18)$$

1.5 The Nuclear-norm Calculation in Eqn. (17)

We assume B and C are 2. In this case, A could be expressed as:

$$A = \begin{bmatrix} x & 1-x \\ y & 1-y \end{bmatrix}, \quad (19)$$

where x and y are variables. To calculate the singular values, we build a new matrix $A \times A^\top$ as follows:

$$A \times A^\top = \begin{bmatrix} x^2 + (1-x)^2 & xy + (1-x)(1-y) \\ xy + (1-x)(1-y) & y^2 + (1-y)^2 \end{bmatrix}, \quad (20)$$

where we could calculate the eigen values of matrix $A \times A^\top$ by:

$$|A \times A^\top - \lambda \mathcal{I}| = 0. \quad (21)$$

Thus we could substitute into the value of $A \times A^\top$ as follows:

$$\begin{vmatrix} x^2 + (1-x)^2 - \lambda & xy + (1-x)(1-y) \\ xy + (1-x)(1-y) & y^2 + (1-y)^2 - \lambda \end{vmatrix} = 0. \quad (22)$$

By integrating the equation, we could obtain the following results:

$$\lambda^2 - 2(x^2 - x + y^2 - y + 1)\lambda + (y - x)^2 = 0. \quad (23)$$

Considering that there are only two singular values in this situation, we denote them as σ_1 and σ_2 . While the solution of the Eqn. 23 is the square of the singular values. Thus we could find that:

$$\begin{aligned} \sigma_1^2 + \sigma_2^2 &= 2(x^2 - x + y^2 - y + 1) \\ \sigma_1 \cdot \sigma_2 &= (y - x)^2 \end{aligned} \quad (24)$$

The sum of the singular values is calculated as follows:

$$\begin{aligned} \sigma_1 + \sigma_2 &= \sqrt{(\sigma_1 + \sigma_2)^2} \\ &= \sqrt{(\sigma_1^2 + \sigma_2^2 + 2\sigma_1\sigma_2)} \\ &= \sqrt{(2(x^2 - x + y^2 - y + 1) + 2|y - x|)} \end{aligned} \quad (25)$$

Then the nuclear-norm could be calculated as:

$$\|A\|_* = \sqrt{x^2 + (1-x)^2 + y^2 + (1-y)^2 + 2|y - x|}, \quad (26)$$

1.6 Maximum of $\|\hat{A}\|_*$

According to inequality of arithmetic and geometric means, we could obtain:

$$\sqrt{a} + \sqrt{b} \leq 2\sqrt{\frac{1}{2}(a + b)}. \quad (27)$$

Then the maximum of $\|\hat{A}\|_*$ could be calculated as follows:

$$\begin{aligned} \|\hat{A}\|_* &= \sqrt{x^2 + (1-x)^2} + \sqrt{y^2 + (1-y)^2} \\ &\leq 2\sqrt{\frac{1}{2}(x^2 + (1-x)^2 + y^2 + (1-y)^2)} \\ &\leq 2\sqrt{\frac{1}{2}(2(\frac{x+1-x}{2})^2 + 2(\frac{y+1-y}{2})^2)} \\ &= \sqrt{2} \end{aligned} \quad (28)$$

where the maximum could be reached when $x = 0.5$ and $y = 0.5$.

2 EXPERIMENT AND ANALYSIS

2.1 SAFN

SAFN [1] is a popular method, which reveals that larger feature norm accompanies with more transferability in the transfer process. While we reanalyze SAFN, and find the intrinsic effect of SAFN is to increase the feature norm towards more prediction discriminability. To show the intrinsic effect, we analyze SAFN from two aspects, *i.e.*, practical view and theoretical view.

From the practical analysis, we gather the results of entropy of source and target predictions during the transfer from $A \rightarrow W$ in Office-31 [2], as shown in Figure 1. The results show that both Source Only and SAFN could achieve high prediction discriminability on source domain. While SAFN

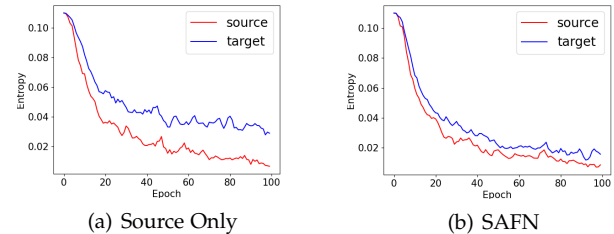


Fig. 1. Statistics of Entropy during the whole training process under Source Only or SAFN. Less Entropy means more prediction discriminability.

could obtain higher prediction discriminability on target domain, compared with Source Only. Thus larger norm tends to accompany with more prediction discriminability.

From theoretical view, we simplify the situation by only one fully connected layer. We denote the feature as $F \in \mathbb{R}^{B \times N_f}$, with N_f dimension. The fully connected layer is simplified as the matrix multiplication with $W \mathbb{R}^{N_f \times C}$ with C categories, and an additional $B \mathbb{R}^C$. Then the category responses A could be calculated as:

$$A = \text{softmax}(F \times W + B). \quad (29)$$

With typical softmax layer, response of A_{ij} could be calculated as:

$$A_{ij} = \frac{e^{(F_i \times W_{:j} + B_j)}}{\sum_{j=1}^C e^{(F_i \times W_{:j} + B_j)}}. \quad (30)$$

When larger norm is achieved as SAFN, the newcomer feature F_i could be approximated as larger feature with multiple variable of n , as follows:

$$F_i' = n \cdot F_i \quad n > 1. \quad (31)$$

Then the newcomer response A_{ij}' could be calculated as:

$$\begin{aligned} A_{ij}' &= \frac{e^{(F_i' \times W_{:j} + B_j)}}{\sum_{j=1}^C e^{(F_i' \times W_{:j} + B_j)}} \\ &= \frac{e^{n \cdot (F_i \times W_{:j} + B_j)}}{\sum_{j=1}^C e^{n \cdot (F_i \times W_{:j} + B_j)}} \\ &= \frac{(e^{(F_i \times W_{:j} + B_j)})^n}{\sum_{j=1}^C (e^{(F_i \times W_{:j} + B_j)})^n} \\ &= \frac{(\frac{e^{(F_i \times W_{:j} + B_j)}}{\sum_{j=1}^C e^{(F_i \times W_{:j} + B_j)}})^n}{\sum_{j=1}^C (\frac{e^{(F_i \times W_{:j} + B_j)}}{\sum_{j=1}^C e^{(F_i \times W_{:j} + B_j)}})^n} \\ &= \frac{(A_{ij})^n}{\sum_{j=1}^C (A_{ij})^n}. \end{aligned} \quad (32)$$

Thus we could find that A_{ij}' is proportional to $(A_{ij})^n$ as follows:

$$\frac{A_{ij}'}{(A_{ij})^n} = \frac{1}{\sum_{j=1}^C (A_{ij})^n} = K. \quad (33)$$

Thus larger n results in larger divergence between A_{ij}' and A_{ik}' for different j and k . Then less entropy and more prediction discriminability could be achieved.

To provide direct comprehension of the effect of SAFN, we construct a toy model where:

$$F = \begin{bmatrix} 0 & 1 & 2 \\ -1 & 1 & 2 \end{bmatrix}, W = \begin{bmatrix} 0 & 1 \\ 1 & 0 \\ 1 & 1 \end{bmatrix}, B = \begin{bmatrix} 0 & 0 \end{bmatrix} \quad (34)$$

Then matrix A could be calculated by Eqn.29:

$$A = \begin{bmatrix} 0.73 & 0.27 \\ 0.88 & 0.12 \end{bmatrix} \quad (35)$$

When $n = 2$, matrix A' could be calculated as follows:

$$A' = \begin{bmatrix} 0.88 & 0.12 \\ 0.98 & 0.02 \end{bmatrix} \quad (36)$$

where we find that the prediction discriminability is higher in A' for each row (sample).

2.2 Semi-supervised Learning

CIFAR-100 [3] is a standard benchmark dataset for semi-supervised learning. We evaluate our method of BNM on CIFAR-100 with 5000 and 10000 labeled examples respectively. We utilize the ResNet [4] model, the same backbone with [5]. The batch size is fixed to 64 in our experiments. The experiments are implemented with Tensorflow [6]. We create 4 splits for each and report the mean and variance across the accuracy on different splits.

The results are shown in Table 1. In semi-supervised learning (SSL), direct entropy minimization could improve the performance, while BNM outperforms entropy minimization. The improvement of BNM applied on a simple pretrained ResNet is moderate compared to other state-of-the-art well-designed SSL methods. However, working with other SSL methods such as VAT [7], BNM demonstrates more significant improvement, which is comparable to methods with more complicated mechanism such as ML+CCN+VAT [8]. Thus BNM is more suitable for cooperation with existing SSL methods, and performs better than entropy minimization in all cases.

TABLE 1
Accuracy(%) on the CIFAR-100 dataset for semi-supervised learning methods.

Method	5000	10000
Temporal Ensembling [9]	-	61.35 \pm 0.51
SNTG+II-model [10]	-	62.03 \pm 0.29
ML+CCN+VAT [8]	56.58 \pm 0.31	64.72 \pm 0.23
ResNet [4]	39.73 \pm 0.33	49.55 \pm 0.28
EntMin	40.92 \pm 0.18	50.36 \pm 0.20
BNM	41.59 \pm 0.27	51.07 \pm 0.24
VAT* [7]	56.63 \pm 0.18	63.62 \pm 0.18
VAT+EntMin	56.97 \pm 0.21	64.48 \pm 0.22
VAT+BNM	57.43 \pm 0.24	64.61 \pm 0.15

2.3 Dataset Balance Comparison

We also compare the number of samples in existing datasets as shown in Table 2. We count the sum of samples (Sum), Mean category number (Mean), Standard category number (Std), Maximum category number (Max) and Minimum category number (Min).

We could find that existing datasets of Office-31, Office-Home, Domainnet and Semi Domainnet contain imbalanced

TABLE 2
Comparisons on numbers of samples for categories.

Dataset	Domain	Sum	Mean	Std	Max	Min
Office-31	Amazon	2817	90.9	13.5	100	36
	Dslr	498	16.1	5.7	31	7
	Webcam	795	25.6	7.5	43	11
Office-Home	Art	2427	37.3	19.6	99	15
	Clipart	4365	67.2	24.1	99	39
	Product	4439	68.3	21.1	99	38
	Real World	4357	67.0	15.8	99	23
Domainnet	Clipart (train)	34019	98.6	55.3	328	8
	Clipart (test)	14814	42.9	23.7	141	4
	Real (train)	122563	355.3	121.0	570	21
	Real (test)	52764	152.9	51.8	245	10
	Painting (train)	52867	153.2	118.1	630	7
	Painting (test)	22892	66.4	50.6	271	3
	Sketch (train)	49115	142.4	97.0	508	9
	Sketch (test)	21271	61.7	41.6	219	4
	Quickdraw (train)	120750	350.0	0.0	350	350
	Quickdraw (test)	51750	150.0	0.0	150	150
Semi Domainnet	Infograph (train)	37087	107.5	94.7	564	8
	infograph (test)	16114	46.7	40.6	242	4
	Clipart	18703	148.4	87.9	469	12
	Real	70358	558.4	142.4	804	147
Balance Domainnet	Painting	31502	250.0	159.4	779	12
	Sketch	70358	558.4	142.4	804	147
	Clipart (train)	6300	50	0	50	50
	Clipart (test)	2772	22	0	22	22
Balance Domainnet	Real (train)	8568	68	0	68	68
	Real (test)	3780	30	0	30	30
	Painting (train)	6804	54	0	54	54
	Painting (test)	3024	24	0	24	24
Balance Domainnet	Sketch (train)	6678	53	0	53	53
	Sketch (test)	3024	24	0	24	24

categories. For example, in Clipart (train) of Domainnet, the largest sample number in categories is 328, while another category holds only 8 samples. Among the domains, only Quickdraw in Domainnet holds 0 Std, other domains attain the value of Std similar to Mean. The large Std means imbalanced category settings, which would inevitably result in prediction bias, with improper conclusions for domain adaptation.

Thus we select samples balanced for the categories selected from Domainnet [11], called Balance Domainnet. In Balance Domainnet, there are four domains including Real (R), Clipart (C), Painting (P) and Sketch (S) with large domain discrepancy. Each domain holds total 126 categories, with at least 50 training samples for each category. To maintain balanced for all the categories, different categories contain the same number of samples for one domain, such as 53 samples for Sketch for training the network.

2.4 Further Discussion

The chosen tasks are typical label insufficient situations to show the mechanism of BNM. Among the tasks and datasets, there are differences in mainly two aspects, *i.e.*, the domain discrepancy and category balance. There exists large domain discrepancy in tasks of domain adaptation and unsupervised open domain recognition, while no domain discrepancy is assumed in semi-supervised learning. From the view of category balance, the categories are balanced in CIFAR-100 of semi-supervised learning. In datasets of domain adaptation, *i.e.*, Office-31 and Office-Home, the categories are imbalanced. While unsupervised open domain recognition is a learning task with extremely imbalanced

category distributions, where some categories are even unseen in the labeled domain. In datasets of I2AwA, 10 categories are unknown categories, which hold a remarkable percentage of the total 50 categories.

As shown in the experiments, BNM could cooperate well with existing methods in semi-supervised learning. For domain adaptation, BNM could outperform most existing adversarial methods. While in unsupervised open domain recognition, method with only the BNM loss and classification loss could even achieve state-of-the-art results. We could see the progressive progress and fitness of BNM to the tasks, from semi-supervised learning to unsupervised open domain recognition. Considering the differences between the tasks, we could obtain two conclusions on the applicability of BNM. The first is that BNM could work well in label insufficient situations. The other is that BNM outperforms entropy minimization significantly, especially when there exists rich domain discrepancy and imbalanced category distribution.

REFERENCES

- [1] R. Xu, G. Li, J. Yang, and L. Lin, "Larger norm more transferable: An adaptive feature norm approach for unsupervised domain adaptation," in *The IEEE International Conference on Computer Vision (ICCV)*, October 2019.
- [2] K. Saenko, B. Kulis, M. Fritz, and T. Darrell, "Adapting visual category models to new domains," in *European conference on computer vision*. Springer, 2010, pp. 213–226.
- [3] A. Krizhevsky, G. Hinton *et al.*, "Learning multiple layers of features from tiny images," Citeseer, Tech. Rep., 2009.
- [4] K. He, X. Zhang, S. Ren, and J. Sun, "Deep residual learning for image recognition," in *Proceedings of the IEEE conference on computer vision and pattern recognition*, 2016, pp. 770–778.
- [5] A. Oliver, A. Odena, C. A. Raffel, E. D. Cubuk, and I. Goodfellow, "Realistic evaluation of deep semi-supervised learning algorithms," in *Advances in Neural Information Processing Systems*, 2018, pp. 3235–3246.
- [6] M. Abadi, P. Barham, J. Chen, Z. Chen, A. Davis, J. Dean, M. Devin, S. Ghemawat, G. Irving, M. Isard *et al.*, "Tensorflow: A system for large-scale machine learning," in *12th {USENIX} Symposium on Operating Systems Design and Implementation ({OSDI} 16)*, 2016, pp. 265–283.
- [7] T. Miyato, S.-i. Maeda, M. Koyama, and S. Ishii, "Virtual adversarial training: a regularization method for supervised and semi-supervised learning," *IEEE transactions on pattern analysis and machine intelligence*, vol. 41, no. 8, pp. 1979–1993, 2018.
- [8] S. Wu, J. Li, C. Liu, Z. Yu, and H.-S. Wong, "Mutual learning of complementary networks via residual correction for improving semi-supervised classification," in *Proceedings of the IEEE Conference on Computer Vision and Pattern Recognition*, 2019, pp. 6500–6509.
- [9] S. Laine and T. Aila, "Temporal ensembling for semi-supervised learning," *arXiv preprint arXiv:1610.02242*, 2016.
- [10] Y. Luo, J. Zhu, M. Li, Y. Ren, and B. Zhang, "Smooth neighbors on teacher graphs for semi-supervised learning," in *Proceedings of the IEEE Conference on Computer Vision and Pattern Recognition*, 2018, pp. 8896–8905.
- [11] X. Peng, Q. Bai, X. Xia, Z. Huang, K. Saenko, and B. Wang, "Moment matching for multi-source domain adaptation," in *Proceedings of the IEEE International Conference on Computer Vision*, 2019, pp. 1406–1415.